



HHS Public Access

Author manuscript

Mol Syst Des Eng. Author manuscript; available in PMC 2018 February 01.

Published in final edited form as:

Mol Syst Des Eng. 2017 February 1; 2(1): 9–33. doi:10.1039/C6ME00083E.

Insights from molecular dynamics simulations for computational protein design

Matthew Carter Childers and Valerie Daggett*

Department of Bioengineering, University of Washington, Seattle, WA 98195-5013, United States

Abstract

A grand challenge in the field of structural biology is to design and engineer proteins that exhibit targeted functions. Although much success on this front has been achieved, design success rates remain low, an ever-present reminder of our limited understanding of the relationship between amino acid sequences and the structures they adopt. In addition to experimental techniques and rational design strategies, computational methods have been employed to aid in the design and engineering of proteins. Molecular dynamics (MD) is one such method that simulates the motions of proteins according to classical dynamics. Here, we review how insights into protein dynamics derived from MD simulations have influenced the design of proteins. One of the greatest strengths of MD is its capacity to reveal information beyond what is available in the static structures deposited in the Protein Data Bank. In this regard simulations can be used to directly guide protein design by providing atomistic details of the dynamic molecular interactions contributing to protein stability and function. MD simulations can also be used as a virtual screening tool to rank, select, identify, and assess potential designs. MD is uniquely poised to inform protein design efforts where the application requires realistic models of protein dynamics and atomic level descriptions of the relationship between dynamics and function. Here, we review cases where MD simulations was used to modulate protein stability and protein function by providing information regarding the conformation(s), conformational transitions, interactions, and dynamics that govern stability and function. In addition, we discuss cases where conformations from protein folding/unfolding simulations have been exploited for protein design, yielding novel outcomes that could not be obtained from static structures.

Keywords

molecular dynamics simulation; computational protein design; enzyme design; thermostability

1. Introduction

Protein design is the creation of proteins either from scratch (*de novo* design) or through the modification of pre-existing structures (protein redesign). Protein design stands in contrast to experimental techniques, such as directed evolution, that generate new proteins by mimicking natural processes. Instead, protein design relies on a combination of chemical and biological intuition; known relationships between sequence, structure, and function; and

*Corresponding author: daggett@uw.edu, Phone: 1.206.685.7420, Fax: 1.206.685.3300.

computational resources to craft proteins. Protein design serves three main purposes. First, it can lead to the generation of proteins that have real-world applications, such as the design of more efficient enzymes to catalyze reactions, or the design of biotherapeutics. Second, protein design serves as a test of our understanding of protein chemistry and protein folding. Third, in the act of designing new proteins, we gain new insights into the determinants of protein structure and function.

Early rationally designed proteins were pioneered in the 1970's by Gutte and coworkers, and include truncated bovine ribonucleases^{1,2}. These designs relied primarily on chemical and biological intuition. Later, as more protein crystal structures became available, computational predictions of secondary structure propensity³ paved the way for the design of elements of protein structure⁴ and topologically simple proteins⁵⁻⁷. Deciphering relationships such as sequence composition, hydrophobic-hydrophilic patterning, and geometric constraints allowed for the design of more complex structures such as Felix⁸ and Betabellin⁹. Richardson and Richardson provide an excellent review of the early days of protein design¹⁰. The 1990s brought increasingly faster computers, enabling the development of more computational tools for protein design, such as side chain rotamer libraries^{11,12}. Over the next decade components of the protein design toolbox were developed, refined, and integrated, we saw the first *de novo* design¹³, the design of a fold not seen in nature¹⁴, and the design of enzymes to catalyze reactions¹⁵.

In recent years, routine access to high performance computing resources, accompanied by refined protein design methodologies, has allowed for the design of increasingly sophisticated proteins with diverse topologies and functions. Other layers of complexity have been added to protein design strategies, including the dynamical nature of proteins, their binding partners, and the interplay between proteins and their environments. Static representations of proteins often mask the critical relationship between dynamics and function. Use of rotamer libraries was an early example of incorporating dynamics into design: allowing residues to sample multiple rotameric states allows for a greater number of potential sequences.

Protein dynamics are present over different spatial and temporal scales: from local fluctuations around equilibrium conformations to large-scale conformational changes upon binding. In most cases, dynamics are intimately connected to protein function. These functional dynamics range from large-scale conformational changes, such as the power stroke mechanism of myosin in muscle contraction¹⁶ to small-scale rearrangements of active site conformations mediated by a network of residues in cyclophilin A^{17,18}. Therefore it is beneficial to incorporate models of protein dynamics and flexibility in designs. When considering more sophisticated designs, especially designs where function is a target, flexibility and dynamics become even more important.

One way to integrate dynamics into protein design is to capitalize on insights from molecular dynamics (MD) simulations. Molecular dynamics uses a physics-based potential energy function, or force field, to simulate protein dynamics as a function of time according to classical Newtonian mechanics¹⁹. While biophysical techniques, such as NMR spectroscopy, can yield insights into protein dynamics²⁰, MD is unparalleled with regard to

the spatial and temporal resolution that it can provide, allowing us to see proteins in action, at least at fast time scales^{21,22}. MD has the power not only to identify functionally relevant conformations, which may be ‘hidden’ to experimental techniques, but it can also provide the details of transitions between these conformations.

No experimental technique is without error or limitation, and molecular simulations are no exception²³. There are three primary sources of error in MD simulations that dictate the extent to which a simulation correctly samples from a thermodynamic ensemble. The first source of error is the accuracy of the force field, an equation used to derive the forces interacting on all of the atoms in a system²⁴. Although force fields have been parameterized empirically, no force field can be truly accurate. However recent force field validations of model proteins have shown that contemporary force fields can reproduce experimental observables^{25–31} and the studies below demonstrate successful MD-derived predictions validated through protein design. The second main source of error is the extent of conformational sampling obtained from the simulation, or the extent to which simulations sample the heterogeneous distribution of conformational states, which is due to constraints on computing time and methods that limit the flexibility and sampling of the protein, as described previously.³² Determining the appropriate length of a simulation is a trade off between economy (shorter simulations) and sampling (longer simulations), constrained by the timescale(s) of the dynamics in question^{33,34}. However, longer simulations are not always better. Numerical errors such as round-off errors and truncation errors propagate as the simulation is extended as a result of numerical integration^{19,35,36}. Specialized integration algorithms and other computational methods for performing simulations have been developed to mitigate numerical error as much as possible^{37,38}, although many of the approaches merely mask the problems through the use of physically unrealistic procedures and scaling of properties yield discontinuous pathways.^{32,39}

As evidenced by the validation of long simulations of BPTI⁴⁰ and ubiquitin⁴¹ the combined errors from force field accuracy, conformational sampling, and numerical integration do not necessarily corrupt the simulated dynamics, but they don’t necessarily provide more information beyond what is obtained in shorter simulations. Overall, advances in force field development^{26–28}, software development⁴², parallelization schemes⁴³, and high performance computing resources⁴⁷ have paved the way for simulations into the millisecond time scale and simulations are getting longer all of the time. Experiment is the ultimate arbiter of the accuracy and reliability of MD simulations. A thorough discussion of error and validation of MD simulations is beyond the context of this review; however, readers are referred to other theoretical and practical discussions of simulation validation^{44–46}. As simulated timescales approach those of experiment and biological relevance, the community can better assess the correspondence of simulation and experiment, and the incorporation of MD-derived predictions in protein design represents another important way to validate the methods.

The validity of protein dynamics derived from MD simulations can be assessed through its use in protein design and MD can inform protein design both directly and indirectly. Direct applications of MD include: the use of insights gained from MD to inform rational design and to generate testable hypotheses that are confirmed through design. Indirect applications include the use of MD: to rank, screen, and evaluate designs; to obtain general insights into

protein dynamics; and to explain relationships between protein dynamics and the molecular mechanisms of protein stabilization. Once the mechanisms are well understood, they can be applied to other designs. Here, we review studies in which conventional MD simulations have been used either directly or indirectly in protein design. We cover three broad areas in which MD simulations have been employed: modulating protein stability, engineering functional regions, and engineering folding/unfolding pathways (Figure 1).

2. Modulating protein stability

The use of natural proteins in biomedical and industrial applications is often limited due to the strict determinants of protein stability^{47–49}. Protein stability is governed by the net sum of forces that determine whether a protein will maintain a native, folded conformation or unfold⁵⁰. Technological applications of proteins may require exposure of the proteins to harsh environments or that the proteins remain stable for extended periods of time. Evolutionary pressure has driven natural proteins toward optimal activity, not stability *per se*, in their native environments. Thus, there have been many examples of proteins that have been mutated leading to increased stability, sometimes at the expense of function^{51–56}. Given that protein stability is not necessarily optimized for native conditions, it is unlikely that proteins are optimized for medical and industrial applications⁵⁷. For example, in the food industry, reactions involving enzymes are often carried out at high temperature to increase the rate and reduce the potential for contamination⁵⁸. However, at elevated temperatures, proteins are susceptible to thermal inactivation due to unfolding or irreversible structural damage⁵⁹. Just as evolutionary pressure has given rise to proteins with optimal function in their native environments, it is possible to design protein variants that remain stable in alternative environments. Theoretical, experimental, and computational studies have identified strategies for designing stable protein variants such as: reducing mobility in flexible regions, introduction of disulfide bonds⁶⁰, introduction of salt bridges⁶¹, and chemical modification of protein structures⁶². However these design strategies are not guaranteed to always work, and they may lead to unexpected results^{56,63}. Instead, judicious selection of design strategies is necessary.

Proteins are inherently dynamic molecules that sample various conformational states beyond those presented in the crystal structures in the Protein Data Bank (PDB)⁶⁴. The ensembles of conformations proteins explore, the transitions between these conformational substates, and the response of these dynamic fluctuations to environmental conditions are coupled to protein stability. In this regard, MD simulations can provide access to atomic details of protein dynamics to aid in the design of stable protein variants.

One of the most common ways to stabilize proteins is to introduce a disulfide bond in the hope of locking down the structure. Increases in protein stability due to the introduction of a disulfide bond have been attributed to lowered entropy of the unfolded state,⁶⁵ enthalpic changes to the unfolded state,⁶⁶ and kinetic stabilization of the folded state⁶⁷. However the introduction of a disulfide can reduce protein stability due to poor packing and flexibility^{68,69} or stabilization of the denatured state.⁶⁰ Thus, it is crucial to identify the optimal sites for the introduction of disulfide bonds and consider the effects of the disulfide bond on nonnative states. One early example focused on incorporation of a disulfide bond

was in haloalkane dehalogenase (DhlA) from *Xanthobacter autotrophicus* and it catalyzes the hydrolytic dehalogenation of small, halogenated alkanes. Pikkemaat et al. used MD simulations of DhlA to identify flexible regions in DhlA that could be stabilized by a disulfide bond⁷⁰. Simulations performed at 298 K revealed a flexible region between residues 180 and 210. This region was classified as inflexible by the crystallographic β -factors. Pikkemaat et al. then used the SSBOND⁷¹ program to identify potential sites for the introduction of a disulfide bond. By cross-referencing sites identified by SSBOND with flexible regions identified from MD simulations, the authors selected residue positions 16 and 201 for the incorporation of a disulfide. Experimental studies followed. The residual activities of the WT protein and designed variants were monitored as a function of temperature and urea. Analogous to the melting temperature, T_m , denaturation transition values were defined as the temperature at which residual activity decreased to 50% of the initial value. The denaturation transition temperatures for the WT, oxidized mutant, and reduced mutant were, respectively, 47.5° C, 52.7° C, and 39.0° C. The design was successful, leading to a variant with an increased activity-temperature profile, but introduction of the Cys residues themselves were quite destabilizing. This study demonstrates the capacity of MD to aid in the rational selection of positions for the introduction of disulfide bonds into proteins. This approach improves on the prediction of amino acid pairs for the introduction of a disulfide bond by factoring in protein flexibility and conformational heterogeneity within the native state and has been used recently by others⁷².

2.1 Stability in harsh environments

The most common method for designing a stable protein variant using data obtained from MD simulations is known as the rigidification of flexible sites⁷³. MD is a convenient way to find such flexible sites, as mentioned above. Simulations at elevated temperatures, initially performed by Daggett and Levitt, were first used to study the mechanisms of protein folding by simulating unfolding pathways,^{74,75} after ensuring that the force field and methods were valid at high temperature^{39,76}. This approach was subsequently validated through extensive comparisons with experiment, including ϕ -values, pioneered by Fersht and coworkers^{77,78}. High temperature unfolding simulations methods have since been employed to design thermostable proteins. The method utilizes MD simulations to directly identify regions of the protein that are susceptible to unfolding by performing simulations at elevated temperatures (Figure 2). Unstable regions are then redesigned through rational design or other computational algorithms, and MD is typically used to test the designs (Figure 2, indirect application).

These methods have been applied in several studies of xylanases, as industrial reactions involving xylanases are often performed at elevated temperatures, which allows reactions to proceed quickly and prevents contamination by microbes⁴⁸. One such example is xylanases, which represent a class of enzymes that degrade the polysaccharide β -1,4-xylan into xylose⁷⁹. They have numerous industrial applications in the pulp, paper, and food industries⁸⁰; however, they are inactivated at high temperature. Xylanases are grouped into families based on their primary and tertiary structures⁸¹. Family 11 xylanases have a single

α -helix and two extended beta sheets, forming a jellyroll fold, and they have been the subject of numerous studies of protein thermostabilization (Figure 3).

To design a thermostable variant of GH11 xylanase from *Bacillus circulans*, Yoo and coworkers first redesigned a flexible surface site and then refined their design using MD simulations.⁸² In the first generation design, a flexible surface cavity was identified by the FRODA⁸³ webserver. Stabilization of this flexible cavity with three mutations (F48Y/T50V/T147L) resulted in a 15-fold increase in thermostability, as measured by $t_{1/2}$ of thermal inactivation in functional assays, and 1.3-fold increase in catalytic efficiency⁸². In a follow-up study, Yoo and coworkers used MD simulations to improve the design by optimizing interactions made by the previously mutated residues⁸⁴ (Figure 3B). MD simulations performed at 300 and 330 K showed that residues N52 and N151 became flexible at high temperature. The RosettaDesign⁸⁵ server was used to predict stabilizing mutations for the flexible residues (N52 and N151) and others that line the redesigned cavity. Five mutations were predicted: I51V, N52Y, T143A, I144V, and T145D to improve stability. Experimental evaluation of single mutant designs revealed that the N52Y mutant had higher residual activity and a longer half-life than the first generation design. The F48Y/T50V/N52Y/T147L quadruple mutant had even higher catalytic efficiency, melting temperature, and resistance to heat inactivation. The increase in thermostability caused by the N52Y mutation was attributed to the formation of a hydrophobic cluster and an aromatic-aromatic interaction between N52Y and W185. Because residues N52 and W185 are conserved in xylanases from multiple species, the authors suggest that the N52Y mutation could be adapted to stabilize homologous xylanases. MD simulations were critical in the identification of the N52Y mutation. Although coarse-grain models of protein flexibility can yield valuable insights, MD provides more detailed descriptions of protein flexibility as well as the details of the interactions that underlie said flexibility.

Another strategy for designing thermostable proteins incorporates insights from the properties of proteins derived from thermophilic relatives. In a survey of the PDB, Argos et al. investigated thermophile/mesophile counterparts from 16 protein folds and concluded that thermophilic proteins are stabilized by an increased number of hydrogen bonds, salt bridges, and surface charges⁸⁶. MD simulations may also be used to infer general principles for protein design. One such application is to compare and contrast the dynamics and stabilities of homologous proteins from mesophilic and thermophilic organisms. Studies from our lab⁸⁷ and others^{88,89} have suggested that thermophilic proteins dynamically adapt to function at higher temperatures due in part to the increased number of polar residues and salt bridges relative to their mesophilic counterparts. Although broad comparisons of thermophilic and mesophilic counterparts can yield general insights into protein design, the true challenge is to decipher the optimal residues to mutate that will improve protein stability without adversely affecting the structure, dynamics, or function of the particular protein in question.

Once stabilizing mechanisms of thermophilic proteins have been identified, it is possible to stabilize their mesophilic counterparts by grafting thermophilic sequences into mesophilic scaffolds. For example, Vieira and Degreve performed MD simulations of a thermophilic xylanase from *Thermomyces lanuginosus* and a mesophilic xylanase from *Bacillus*

*circulans*⁹⁰. They used MD simulations to compare residue flexibility and salt bridge occupancy between TLX and BCX at temperatures between 25° and 70° C. TLX has a larger number of intramolecular interactions among residues in the ‘fingers’ domain as well as more favorable interactions between side chains and solvent. Building off of the results from Vieira et al.^{90,91}, Alponi et al. grafted charges from a thermophilic GH11 xylanase into a mesophilic scaffold⁹² (Figure 3C). In total, five mutations were made in the ‘fingers’ domain: S22E, S27E, N32D, N54E, N181R. These five single amino acid mutants were used in an experimental combinatorial library, yielding the S22E/N32D mutant, which displayed higher stability than the WT and single mutant designs. The S22E/N32D mutant had 1.9 fold higher specific activity (WT: 25.0 U mg⁻¹ vs. S22E/N32D: 46.9 U mg⁻¹ where U = activity units), with a $t_{1/2}$ of thermal inactivation 6.3 times that of WT (WT: 13.3 min vs. S22E/N32D: 84.8 min). Comparisons of thermophilic and mesophilic homologue dynamics also led to the design of a thermostable variant of nitrile hydratase (NHase)⁹³. By grafting thermophilic sequences into a mesophilic homologue, the resulting designed protein had enhanced thermal stability relative to WT.

Successful design of more stable proteins is not limited to enzymes. Repeat proteins, proteins with modular scaffolds, consist of repeated elements of a fundamental building block of structure. Ankyrin repeat proteins consist of repeats of a 33-residue helix-loop-helix-loop motif^{94,95}. The development of highly stable variants of repeat proteins was accomplished using the consensus design approach,⁹⁶ by which homologous sequences were compared to determine the optimal residues at each position in the repeat unit⁹⁷⁻⁹⁸. To improve the thermostability of designed ankyrin repeats, Caflisch and co-workers combined equilibrium unfolding experiments and high temperature MD simulations to investigate the effects of the number of repeats on stability⁹⁹. They modeled ankyrin repeats of the form NI_xC, where I_x refers to the number of internal consensus repeats, and N and C refer to the N- and C- terminal capping repeats, respectively. Native state simulations (300 K) of NI₁C, NI₂C, and NI₃C showed that a network of salt bridges formed at inter-repeat interfaces stabilized the proteins. High temperature unfolding simulations (400 K) showed that NI₁C and NI₂C unfolded while NI₃C retained a native-like conformation, in agreement with experiments showing a correlation between thermal stability and the number of repeat units. Additional unfolding experiments showed that NI₄ is more stable than NI₄C and has two-state folding characteristics, but is less soluble and more prone to aggregate. This suggested an opportunity to redesign the internal I:C interface to strengthen inter-repeat interactions while simultaneously providing the aggregation-disfavoring properties of the cap. In total, six redesigns of NI₁C were made, each with between two and 11 mutations grouped into three categories: mutations to redesign the hydrophobic interface, mutations to facilitate hydrogen bond formation, or mutations to elongate the second helix of the C-terminal. Subsequent high temperature MD simulations of the designs predicted that the hydrophobic mutations did not significantly contribute to protein stabilization while the hydrophilic and helix elongation mutations did. Thermal unfolding experiments confirmed that the introductions of hydrogen bond-promoting mutations and helix-elongating mutations stabilized the protein, as evidenced by an increase in the T_m from 60°C for WT to 77°C for one of the designs. MD simulations were essential in the identification of residues at the interface where mutation would be most beneficial.

To design proteins for increased stability in other environments, the general strategy remains the same; however, instead of performing simulations at elevated temperatures, the simulation conditions are set to mimic the environment where enhanced stability is desired. For example, to design pH stable protein variants, simulations are performed at different pH levels by modifying the protonation states of titratable residues. For example, armadillo repeat proteins were designed using a consensus method, but NMR revealed unfavorable interactions at neutral pH that were absent at high pH. A pH stable variant was designed by mutating Lys residues to Gln based on MD simulations¹⁰⁰.

Mutations involving titratable side chains can modulate pH-dependent protein stability¹⁰¹. Penicillin acylase from *Escherichia coli* and other members of the Ntn-hydrolase superfamily¹⁰² cleave amide bonds^{103,104}. Members of this family have diverse pH stability profiles and *E. coli* penicillin acylase becomes inactive at acidic or alkaline pH¹⁰⁵. Suplatov et al. combined sequence analysis with constant pH MD simulations to design a pH stable variant suitable for industrial applications¹⁰⁹. At neutral pH two residues in the B1 domain, Glu482 and Asp484, share a proton and coordinate a hydrogen bond network that stabilizes the active site. At alkaline pH, when both residues are negatively charged the hydrogen bond network collapsed. The authors attributed the pH-mediated inactivation of the enzyme to the loss of the active site conformation. They then took this a step further and aligned the sequence of penicillin acylase from *E. coli* to penicillin acylase from *Alcaligenes faecalis*, which does not become inactive at alkaline pH. A potential mutation, D484N, was suggested by cross-referencing the MD-derived mechanism of instability at alkaline pH with potential mutations identified by inferring mutability from the sequence alignment. Simulations of the D484N of *E. coli* protein at neutral pH were comparable to those of the WT but the mutant was stabilized at alkaline pH, as predicted. Experimental follow-up confirmed that the inactivation rate decreased 9 fold for the mutant relative to WT.

Simulations of nonnative environments can also be combined with elevated temperature simulations. For example, to engineer a pH stable variant of the sweet protein MNEI, Leone and Picone performed MD simulations at native and elevated temperature and for various protonation states of Glu 23¹⁰⁶. When E23 was protonated, the simulations remained stable over a range of temperatures. Protonated E23 contributed to overall stability through formation of a hydrogen bond network that was disrupted when it was deprotonated. A pH-stable variant was designed by mutating E23 to Q, and the melting temperature increased by ~10° C at both neutral and alkaline pH without altering stability at low pH. With careful modeling of the desired conditions and the selection of appropriate controls, MD is able to simulate many environments. Once potential design sites have been identified from MD simulations, it is possible to combine the results with a long list of established protein design strategies, including performing simulations at high temperature.

2.2 Post-translational modifications and non-standard amino acids

As mentioned above, post-translational modifications (PTMs) and non-standard amino acids represent another route to stabilize proteins and regulate function¹⁰⁷. Of the over 25 distinct PTMs that have been experimentally identified, phosphorylation, acetylation, and N-linked glycosylation are the most frequent, and extensive databases allow for routine access to

statistics and properties of PTMs^{118,110}. It is possible to introduce or remove PTMs into proteins through the modulation of sequence motifs (e.g. N-X-T/S for N-linked glycosylation).

More than half of all proteins are predicted to be glycosylated¹¹¹. Protein glycoengineering is accomplished by the introduction or removal of glycosylation sequences at specific sites in proteins^{112,113}. Glycosylation can be incorporated into protein design to confer advantageous properties, such as increases in *in vivo* half-life and stability, burial of hydrophobic patches, decreases in aggregation, and increasing solubility¹¹⁰. In pharmaceutical formulations of interferon- β , solvent-exposed hydrophobic residues drive the formation of protein aggregates, rendering the protein non-functional. The majority of designed proteins have focused on making mutations to favor a specific conformation or function, i.e. positive design; however, in some cases it is necessary to make designs that prevent access to particular interactions, conformational states or functions, i.e. negative design^{114,115}. To reduce the aggregation propensity of interferon- β , Samoudi et al. used negative design to create hyper-glycosylated variants of interferon- β . MD simulations were used to evaluate the designs by comparing the structure, dynamics, residue flexibility, and solvent flexibility of the designed glycosylation sites to WT¹¹⁶. Glycosylation sites were selected by combining web server predictions, a literature search, and structure-based design from available crystal structures. By comparing the flexibility of designed, glycosylated proteins with wild type (WT), two models were selected for experimental characterization, which confirmed hyper-glycosylation and retention of function. Negative design can also be used to avoid conformations and functions such as off-pathway folding intermediates, conformational substates of the native ensemble, protein-protein interactions, protein-ligand interactions, aggregation-prone states, and pathological states such as amyloid. High temperature MD simulations have also been used to generate reference structures for 'negative states'¹¹⁷.

In an example of the use of MD in this area, Fonseca-Maldonado and Ward investigated the relationship between the pattern of glycosylation and xylanase thermostability by systematically modulating the pattern of glycosylation¹¹⁸ (Figure 3D). GH11 xylanase from *Bacillus subtilis* has 6 putative glycosylation sites (N8, N20, N25, N29, N141 and N181) and in WT, 4 sites were glycosylated (N20, N25, N141 and N181) when expressed in *Pichia pastoris*¹¹⁸. Fonseca-Maldonado and Ward systematically mutated Asn residues to Gln in order to generate mutants with different patterns of glycosylation. By correlating glycan-protein, glycan-glycan, and protein-protein interactions observed *in silico* to experimental measures of stability, they showed that both the pattern and extent of glycosylation contributed to protein stability. In general, glycosylation improved stability; however, the number and pattern of glycosylation sites finely tunes protein stability. For example, the most stable protein in this study had three of five glycosylation sites occupied. Additionally, removal of some glycosylation sites allowed previously unoccupied sites (8 and 29) to become occupied. MD simulations were also used to explain why more glycosylation does not always increase stability, as well as the molecular mechanisms behind glycosylation and stability.

Another technique to expand the repertoire in the computational design of proteins is to use non-standard amino acids. Non-standard amino acids are amino acids other than the twenty common amino acids coded for by DNA. The ability to incorporate non-standard amino acids, such as D-amino acids, and PTMs into designed proteins greatly increases protein design space and offers alternative strategies for designing stable proteins. One such opportunity is to use D-amino acids to stabilize unfavorable ϕ/ψ backbone dihedral angles. The left-handed α -helical (α_L) region of ϕ/ψ space is rarely populated in 'normal' globular proteins, and is generally an unfavorable conformation for non-Gly L-amino acids¹¹⁹. In contrast to L-amino acids, D-amino acids have greater preference for α_L conformations and the right-handed α -helical (α_R) region of ϕ/ψ space is disfavored¹²⁰. Rodriguez-Granillo et al. hypothesized that mutation of a C-terminal helix capping Gly residue to a polar D-amino acid could stabilize the α -helix of Trp-cage version 5b¹²¹. A D-amino acid in the α_L conformation at a C-terminal helix capping position additionally allows for helix stabilization through the formation of a hydrogen bond between the side chain of the D-amino acid and the backbone of the helix. They first mutated G10 to bulkier L-amino acids, G10A and G10Q, at the C-terminal end of the α -helix and found that these mutations were destabilizing by MD. Next, they focused on D-amino acid mutations at this position G10a, G10n, and G10q (where lowercase is used for D-amino acids). They found that the extent of fluctuations and hydrogen bond occupancies at the mutation site correlated with stability. However, they also found that the D-Ala mutation did not increase stability; thus, the magnitude of gains in stability is, not surprisingly, dependent on both the backbone chirality and side chain properties of the amino acid. In addition to their use in helix capping, D-amino acids have also been incorporated into the design of stable β -turns¹²², α -sheet peptides to inhibit amyloid formation,^{123,124} design of novel protein folds^{125,126}, stabilization of large proteins¹²⁷, and stabilizing β -hairpins¹²⁸.

2.3 Tradeoffs between stability and function in design

Candida antartica lipase B catalyzes a variety of organic reactions¹²⁹, and it is used in numerous industrial applications due to its enantioselectivity and wide range of substrates. One need for a thermostable variant of *C. antartica* lipase B is in biodiesel production. To aid in the design of thermostable variants of *C. antartica* Lipase B, Park et al. performed MD simulations at four different temperatures: 300, 330, 360, and 400 K¹³⁰ to determine vulnerable regions of the structure. Park et al. used the rigidification of flexible sites method to design thermostable variants. The designs were tested experimentally by determining their specific activities and residual activities. A T158S mutant had 2× the specific activity of WT whereas the A251E mutant had 0.5× the specific activity of WT. The WT, T158S, and A251E designs showed 55%, 44%, and 75% residual activity after 4–5 hours, respectively. The results of their designs showed an important tradeoff. The mutant most susceptible to thermal denaturation (T158S) had the highest specific activity under native conditions, while the design with the lowest specific activity (A251E) retained its activity for longer periods of time at elevated temperatures. Similar negative correlations between protein stability and function have been observed for mutants of dihydrofolate reductase,⁵¹ the Hesx-1 DNA binding domain,^{52,131} prolactin^{53,132}, troponin C⁵⁴, and a M2 transmembrane proton channel⁵⁶. However the relationship between protein thermodynamic stability, function, and flexibility is complex: positive correlations between stability and function have been

reported for human fibroblast growth factor 1¹³³ and calbindin D_{9K}^{134,135}. These conflicting results suggest that systems respond to mutations in distinct ways. This highlights an important design consideration: often multiple objectives must be balanced. Importantly, designs that increase protein stability should also avoid changes that disrupt the native fold, dynamics, or functional regions of the design.

3. Engineering functional regions into proteins

Functional sites in proteins include active sites, ligand binding sites, and protein-protein interaction sites. Proteins depend upon coordinated dynamics of these sites to perform their functions. It is often desirable to engineer these regions of proteins in order to optimize the activity of natural proteins or to introduce new functionality into existing protein scaffolds.

3.1 Designing binding sites

The design of protein-protein and protein-ligand binding sites is challenging due to the large surface areas involved, their conformational flexibility, and the interplay of solvent and protein dynamics at the sites^{136,137}. There are two overarching design strategies for engineering binding sites. The first is to engineer the binding site for enhanced protein:ligand or protein:protein interactions by mutating residues that are directly involved in the interaction. The second strategy is to alter the conformational diversity of the binding site by mutating residues that drive the stabilization of alternate conformational states. By resolving details of the interactions that favor or disfavor binding and by identifying residues that regulate binding site geometry, MD simulations can provide a wealth of details to guide design.

Given its dynamic nature the 13-residue peptide compstatin has been the subject of numerous MD design efforts. This peptide inhibits the cleavage of human C3¹³⁸ and has potential therapeutic use as a treatment for unregulated complement activation¹³⁹. It is active against C3 from several primate species, but not in lower mammals¹⁴⁰, such that rodents are poor disease models as human compstatin does not interact with rat C3. To create a viable rat model for evaluating compstatin as a therapeutic, Tamamis et al. capitalized on MD simulations to design a ‘transgenic’ rat C3 protein that binds human compstatin and retains its other functions¹⁴¹. The crystal structure of the complex between C3c and an acetylated double mutant of compstatin¹³⁸ (Ac-Val4Trp/His9Ala, henceforth ‘W4A9’), which is more active than WT compstatin, served as the starting conformation for MD simulations. The static structure of the complex sheds little light on the improved activity of W4A9 against compstatin or why human compstatin fails to inhibit cleavage of C3 in lower mammals. MD simulations were performed of the complex between W4A9 and truncated human C3c, the complex of W4A9 and truncated rat C3c, and free human C3c¹⁴², resulting in four specific regions in human C3c with strong interactions with W4A9. In the rat C3c:W4A9 complex, local conformational changes proximal to the compstatin binding site distorted the structure of the binding site and eliminated or reduced intermolecular interactions between rat C3c and W4A9. Two transgenic designs were created in which the positions mostly likely to introduce W4A9 binding competency in rat C3 were selected on the basis of interactions that were lost or destabilized in the rat:W4A9 simulation. In this example, it was important

to balance two design constraints. First the binding region was humanized to promote compstatin:C3 interactions; second, the structural scaffold was preserved to retain rat-like characteristics. Subsequent MD simulations of the humanized designs showed increased interactions between rat C3 and the W4A9 compound. Insights from this paper also aided in the design of compstatin analogues by the same group¹⁴³. This work demonstrates how MD simulations can be used to engineer a binding site to interact with a nonnative ligand and highlights the fact that the goals of a designed protein must be balanced against other objectives, such as the retention of other interactions in the designed protein.

Cytochrome b₅ (cyt b₅) is a heme-containing protein that participates in electron transfer reactions and can interact with multiple proteins. MD simulations of cyt b₅ demonstrated that collective motions of surface residues of cyt b₅ resulted in the transient exposure of a hydrophobic cleft on the surface of the protein¹⁴⁴ (Figure 4). While short by today's standards, this study was the longest simulation at the time and it was cited as the first time a simulation had significantly deviated from the starting position and returned,¹⁴⁵ and prior to this deviations led to irrecoverable changes and there was the fear that numerical errors would spoil long simulations. Furthermore, with respect to the substates sampled, both the open form, discovered by MD, and the closed form, observed in crystal and NMR structures, are consistent with solution NMR data. Based on the proximity of the cleft to residues implicated in protein-protein recognition, it was proposed that cleft dynamics regulate protein recognition as well as access to the heme through the cleft. In a follow up study, Storch et al. then engineered Cytochrome b₅ to alter cleft dynamics¹⁴⁶. They created two designs to inhibit cleft formation. In the first design a single mutation, S18D, introduced a salt bridge across the site of cleft formation. In the second design, a disulfide bond was introduced at positions 18 and 47, across the cleft. In this way the formation of the cleft, and subsequent access to the heme, could be controlled by reducing the disulfide bond or breaking the salt bridge. Subsequent MD simulations confirmed that the designs prevented the opening and closing of the cleft (Figure 4). Follow-up experimental studies employing a variety of techniques, most notably NMR, verified the formation of the cleft as well as the effects of the mutations designed to rationally control cleft formation.¹⁴⁷ This study demonstrates the power of MD simulations to reveal functionally relevant conformations that are excursions from the static, averaged experimental structures, as well as the molecular motions that control exchange between alternate conformations.

Later, de Groot and coworkers used a similar approach to shift the conformational equilibrium of ubiquitin¹⁴⁸. Ubiquitin populates both an open and closed state and dynamically fluctuates between the two via a pincer-like motion. Ubiquitin's many binding partners preferentially interact with one of the two states. de Groot and coworkers engineered ubiquitin to skew the conformational preferences such that one state was more populated than the other to obtain selective binding¹³⁸. To do this MD simulations of unbound ubiquitin were performed to identify the most promising mutations to alter the populations of the two states. Umbrella sampling simulations were subsequently used to construct free energy profiles of the pincer mode, and 11 out of 15 proposed mutations shifted the conformational equilibrium towards one state over another. They then evaluated binding properties experimentally and confirmed their computational predictions.

3.2 Designing enzyme active sites

Enzymes are attractive catalysts because of their efficiency, selectivity, specificity, and biodegradability⁵². However, there is a limited number of naturally occurring enzymes, which can limit the feasibility of using natural enzymes as catalysts in technological applications. Computational design seeks to overcome this limitation by engineering enzyme efficiency, stabilizing naturally occurring enzymes, and designing enzymes to catalyze arbitrary chemical reactions.

P450 TxtE from *Streptomyces scabies* is an enzyme from the cytochrome P450 superfamily that regioselectively catalyzes aromatic nitration¹⁴⁹. These enzymes rely on dynamic rearrangements of the B/C and F/G loops, which seal the active site upon substrate binding, to regulate the high reactivities of reaction intermediates. Arnold and coworkers obtained crystal structures of P450 TxtE that revealed a functional role of the B/C loop; however, they were unable to determine the interactions made by the F/G loop, as it is disordered in the crystal structure¹⁴⁹. Computational approaches were used to model the structure and dynamics of the disordered F/G loop¹⁵⁰. First, the F/G loop was constructed via homology modeling followed by short MD simulations. Snapshots were taken from the trajectories at regular intervals and subjected to geometry optimization. Of these snapshots, the Top 100 energetically favorable structures were used as starting points for production MD.

The transition from a disordered state to an ordered closed state occurs on long time scales. To circumvent this computational bottleneck and to avoid biasing the results via enhanced sampling schemes, Arnold and coworkers used multiple rounds of adaptive sampling to exhaustively simulate the open-to-closed transition (Figure 5). The combined production runs were used to construct coarse-grained and fine-grained Markov models of the transition. The coarse-grained model encompassed 9 unique conformational states, i.e. macrostates. The fine-grained model contained many microstates whose conformations differed by small amplitude changes (such as side chain rearrangements).

The Markov state models were used to organize the trajectories into discrete conformational states and to identify the connectivity of the conformational states, resulting in a predicted transition mechanism of the F/G loop from an open, disordered conformation to a closed, ordered conformation (Figure 5). A single conformational state was observed in all transitions and had characteristics of both the bound and unbound macrostates. This conformational state was defined as the transition state of the closing and opening of the F/G loop. In the closed state, Y175 forms an interaction with Y89; in the transition state H176 interacts with Y89 as opposed to Y175. These results suggested that mutation of H176 could be used to stabilize the closed state of the FG loop in the presence of substrate. Two mutations, H176Y and H176F, were tested experimentally and resulted in 15- and 8-fold higher binding affinities, respectively, and produced 5-nitro-L-tryptophan (5NT) instead of 4-nitro-L-tryptophan (4NT). Additional mutations at these positions modulated the production of 5NT and 4NT. The WT produces 4NT. The WT protein (H176) produced 4NT; designs with N, G, S, or M at position 176 produced a mix of 4NT and 5NT; and designs with F, Y, or W at position 176 produced 5NT. Simulations of the His176 mutations with aromatic residues (F, Y, or W) also demonstrated a stabilization of the closed conformation of the F/G loop. Crystal structures of designs with an aromatic mutation at

position 176 had fully resolved F/G loops in the closed state. For some proteins, such as TxtE, simulations on the microsecond – millisecond timescale may be necessary to resolve the functional dynamics. For other proteins simulations on the nanosecond – microsecond timescale are sufficient. It may be difficult to know *a priori* the time scale necessary to capture functional dynamics, but in general the processes of interest are quite fast with long waiting times determining the timescale. In such situations performing many independent short trials can increase the odds of observing conformational changes beyond the simulation timescale while still maintaining unbiased dynamics.¹⁵¹

The Kemp elimination reaction, i.e. the deprotonation of carbon, is a well-characterized reaction for which no known naturally occurring enzyme exists¹⁵². Several groups have designed novel enzymes to catalyze the reaction^{153–156}. Building off of the successes of other designed Kemp eliminases, Mayo and coworkers combined the “inside out” design method of Zanghellini et al.¹⁵⁷ with MD simulations to iteratively design a Kemp eliminase¹⁵⁸. Xylanase from *Thermoascus aurantiacus* was used as the scaffold in the first generation design, HG-1. Seven mutations were made to the scaffold to create the Kemp eliminase. Designs in the active site were inspired by prior Kemp eliminase designs from Roethlisberger et al.¹⁵³ and the catalytic antibody 34E4^{154,159}. Although HG-1 did fold to the designed structure, it did not demonstrate any Kemp eliminase activity. To understand why the design showed no activity, Mayo and coworkers determined the crystal structure of HG-1 and performed MD simulations. The crystal structure showed that two of the active site residues were rotated out of the active site, which prevented substrate binding and exposed the active site to solvent. MD simulations performed in the presence and absence of substrate showed that the active site was too exposed to solvent and that the active site residues had a high degree of flexibility. Furthermore, the simulations predicted that the active site explored conformations that were inconsistent with the initial design and incompatible with catalytic function. In the second-generation design, HG-2, Mayo and coworkers redesigned the active site to increase its size, hydrophobicity, and burial in the protein. MD simulations of HG-2 suggested that it should be active, although two distinct conformations of the active site were populated during the simulation. Subsequent experiments confirmed that their design was active, with a catalytic efficiency comparable to that of the best designs of Roethlisberger et al.¹⁵³. Additional analysis of the HG-2 simulations suggested that the alternate binding mode was more populated than the designed conformation and had a greater potential for catalytic activity. In the third generation design, HG-3, an additional mutation (S265T) was made to decrease the flexibility of active site residues, to reduce the conformational heterogeneity of the active site, and to promote the alternate conformation. Simulations of HG-3 confirmed a loss of conformational heterogeneity in the active site. Experimental evaluation of HG-3 showed higher catalytic efficiency than any of the previous designs, demonstrating the added value of incorporating MD with other design methods (Figure 5).

MD simulations have also been used to understand the shortcomings of designs to catalyze the Retro-Aldol reaction. Jiang et al. created *de novo* designs to catalyze the multi-step Retro-Aldol reaction¹⁶⁰. In that study, 32 out of 72 reported designs showed Retro-Aldolase activity; however, the best performing designs from that study had rate enhancements 2–3 orders of magnitude lower than catalytic antibodies^{15,161}. To investigate whether the

geometric criteria for Retro-Aldolase activity were maintained, Ruscio et al.¹⁶² performed MD simulations of RA22 from Jiang et al.¹⁶⁰ in complex with substrate. The simulations revealed that two substrate orientations were possible and that two geometric criteria, corresponding to the nucleophilic attack and proton abstraction steps in the Retro-Aldol reaction, were satisfied only ~50% and ~25% of the time during simulations, and thus only rarely were both criteria met simultaneously. Ruscio et al. suggested that explicit exclusion of protein and ligand flexibility during the design process concealed the inability of the designs to maintain productive active site geometry. They attributed the low rate enhancements of the designs to the inability of the active site to maintain the designed geometry. Later, Baker and coworkers refined another Retro-Aldol design, RA34, using directed evolution¹⁶³. The refined RA34.6 variant had higher catalytic efficiency, but structural studies revealed some persistent design flaws. Namely, the flaws were increased conformational heterogeneity of catalytic lysine residue and heterogeneity of the substrate within the binding pocket. These shortcomings are quite similar to those suggested by the MD simulations of Ruscio et al.¹⁶²

3.3 Screening and ranking computational designs

Natural enzymes are usually orders of magnitude more efficient than even the best designed proteins. Furthermore, designed enzymes with high sequence identity can have drastically different catalytic properties. A challenge in protein design is to successfully distinguish active from inactive designs and to rank active designs. By providing atomic details of active site conformations and dynamics, MD simulations have the capacity to aid in the screening and ranking of enzyme designs¹⁶⁴. Simulations of potential designs are screened according to pre-determined metrics, e.g. the stability of active site conformations, and top performing designs for refinement or experimental characterization. For example, Houk and coworkers were not able to differentiate between active and inactive Kemp eliminase designs using quantum mechanics (QM) cluster models and full enzyme QM/MM and PM3/PDDG/MC calculations¹⁶⁵. The major problem was that these approaches cannot model changes in protein structure and solvent accessibility accurately. They then performed MD simulations of Kemp eliminase (KE) with and without substrate, and tested whether the active site geometry was preserved in 23 KE designs using cathepsin K and catalytic antibody 34E4 as references. Designs were predicted to be inactive if active site geometries deviated from the designed conformation. The activity of 20 out of 23 designs was predicted correctly. In another example, Bjelic et al. used QM and MD simulations to design a protein to catalyze the slow, multistep Morita–Baylis–Hillman (MBH) reaction¹⁶⁶. The MD simulations predicted designs with stable active site conformations, which were subsequently confirmed experimentally. Privett et al.¹⁵⁸ also used MD simulations to predict whether active site “recapitulation” designs would be active using similar criteria to those used in Kiss et al.¹⁶⁵. MD simulations successfully predicted the activities of five out of six designs. These studies demonstrate the utility of MD for evaluating designs as a filter for the design process.

4. Design insights from unfolding / folding pathways

Protein folding is a complex process by which an unfolded polypeptide chain adopts a well-defined, compact structure. Protein folding begins at the denatured state, which can contain

varying degrees of dynamic residual secondary and/or tertiary structure. The polypeptide chain proceeds through a series of intermediate states before arriving at a native, folded state. The relationship between sequence and structure is complex, as highlighted by the heteromorphic proteins G_A and G_B , which have high sequence identity (77–98%), but distinct topologies^{169,170}. The solution to this conundrum came through MD-derived predictions that interactions in the denatured state determined whether the α -helical G_A fold or β -grasp fold of G_B would be adopted¹⁶⁹. These MD predictions were later confirmed by experiment¹⁷⁰. Thus, atomic details of protein folding that are often hidden or obscured by experimental techniques can be revealed by MD simulations. Conventional MD simulations of *ab initio* protein folding with full atomic resolution remain computationally intense, even for very small proteins. As an alternative to *ab initio* folding simulations, less computationally intensive techniques, such as high temperature MD, have been developed to sample protein unfolding/folding pathways^{74,75} and microscopic reversibility has been demonstrated.^{171,172} Predictions about the folding/unfolding mechanism of a protein, whether they are obtained from experiment or simulation, can be tested through protein design. Once such mechanisms have been characterized, protein design may then be used to alter the kinetics and thermodynamics of folding pathways.

4.1 Designing fast folding protein variants

The first design based on a simulated protein unfolding / folding pathway focused on the transition state, paving the way for the design of faster folding proteins. This study entailed high temperature simulations to obtain the unfolding pathway of chymotrypsin inhibitor 2 (CI2)¹⁷³. The transition state of unfolding/folding was predicted by conformational clustering and subsequently validated by experiment^{78,174–175}. For a high temperature unfolding simulation, the putative transition state (TS) ensemble of folding/unfolding can be identified using conformational clustering^{171,176}. In this technique, the C_α root mean squared deviation is calculated between all structures in the trajectory and placed into a $N \times N$ matrix. Then the matrix is reduced to a $3 \times N$ dimensional matrix using a dimensionality reduction algorithm. This set of points is then viewed as a 3D trajectory with sequential points connected in time and with the trajectory clustered by conformational similarity. The TS is predicted to be the when the protein leaves the native cluster (Figure 6). Analysis of the MD-derived TS using this method revealed two regions of CI2 with unfavorable nonnative interactions.¹⁷⁵ We reasoned that mutations that minimize these unfavorable interactions in the TS would accelerate folding provided they did not also stabilize the native or denatured states. In this way, the MD simulations were extremely useful because the interactions were evaluated in all WT states and the designed mutations were also simulated prior to experimental validation. The first region identified for redesign was at the C-terminus of the α -helix. In the native state, D23 forms a salt bridge with K2. In the TS, the unpaired D23 made unfavorable interactions with the helix dipole, specifically the unpaired backbone carbonyl group at the C-terminus of the α -helix. The D23A mutation was made to relieve charge repulsion and made use of a helix-promoting residue. The second region was the protease-binding loop, which became distorted in the TS, resulting in charge repulsion between the three Arg residues that are normally involved in interactions with the main chain in the native state (Figure 6). A multiple sequence alignment between CI2 and 18 homologous proteins showed that both R46 and R48 are highly conserved, but that Phe was

observed at position 48 in two homologues and Trp was observed at position 48 in one homologue. The R48F mutation was selected and predicted to increase the folding rate by removal of unfavorable electrostatic interactions. Experimental studies supported the predictions and both mutants folded more rapidly than WT, and R48F yielded that fast folding CI2 variant with nearly two orders of magnitude improvement in the rate of folding (Figure 6). MD was critical to achieve this result since knowledge of both native and nonnative interactions of the TS and denatured state was necessary.

Later, Piana et al. used a similar approach to design a faster folding FiP35 WW domain¹⁷⁷. An *ab initio* folding simulation of the FiP35 WW domain⁴⁰ was used to construct the folding pathway of the FiP35 WW domain. They capitalized on knowledge of residual structure in the unfolded state, rate limiting steps to hairpin formation, and structure of the transition state ensemble to design a faster folding variant, which they subsequently validated experimentally.

Myoglobin is heme binding protein and a member of the globin fold family and has 8 α -helices arranged in two hydrophobic cores: ABGH (formed by helices A, B, G, and H) and CDEF (formed by helices C, D, E and F). In the absence of the heme prosthetic group, apomyoglobin (ApoMb) adopts a fold similar to the native structure of holo-myoglobin¹⁷⁸. The CDEF domain contains more local contacts and it was expected to fold prior to the ABGH domain. Despite these predictions, stopped flow refolding experiments showed that in the absence of heme, the ABGH domain forms rapidly, followed by formation of CDEF^{179–181}. This unexpected behavior was attributed to the stabilization of the CDEF hydrophobic core by heme. Grubele and coworkers increased the speed of folding of the CDEF domain by using MD simulations to design apomyoglobin variants with well-packed hydrophobic cores in the absence of heme¹⁸². Two initial mutants were introduced that were obtained from the literature that lead to greater stability, secondary structure content, and faster folding of CDEF: H64F and P88A^{183,184}. Three additional mutations were made that reduced cavity volume and increased hydrophobic interactions in the heme cavity: L89W, V68W, I107M. In total, five variants were simulated and experimentally tested. The heme cavity in the WT protein has a void volume of 638 Å³. MD simulations showed that as the number of hydrophobic mutations increased, so did the reduction in cavity volume, up to 21%. These mutations also increased the size of the side chain residue interaction network connecting the C, D, and E α -helices. The ApoMb-3, 4, and 5 designs had ~20% greater helix content than WT, as monitored by CD. All ApoMb designs had melting temperatures approximately 20°C higher. Finally, stopped flow refolding measurements showed that two of the mutants refolded four times faster than WT.

4.2 Stabilizing nonnative and intermediate states of proteins

MD also proved to be instrumental in characterizing the folding/unfolding pathway of the engrailed homeodomain (EnHD). This simple 3-helix bundle protein is particularly interesting because it is an ultrafast unfolding and folding protein, allowing the time scale of the process by MD to be probed directly at experimentally accessible temperatures in a collaborative study between the Daggett and Fersht groups. In temperature-jump experiments, EnHD folds to an intermediate state in 1.5 μ s and the transition from I to N

takes ~15 μ s. The relaxation kinetics were followed to 338 K and extrapolated to 348–373 K.¹⁸⁵ The thermal unfolding of EnHD was also investigated at a variety of temperatures and the time taken to reach the TS in the simulations is in agreement with the unfolding times determined experimentally (Figure 7), and the simulations were done as predictions 3 years prior.¹⁸⁶ The TS of EnHD contains native-like secondary structure and a partially packed hydrophobic core. The calculated and experimental Φ -values for the TS, using the method described above for CI2, are in good agreement ($R=0.85$, Figure 7), and again the MD preceded the experimental study.^{187,188} The simulated unfolding process is independent of temperature, and essentially the same TSs are obtained at 348, 373, and 498 K.^{189,190} Higher temperature accelerates the process without changing the overall pathway. By MD, from the TS, reorientation of the helices, expansion and disruption of the helix docking leads to the intermediate. This intermediate has a high helical content and few tertiary contacts (Figure 7).^{185–187} Five years later the structure was determined directly by NMR,¹⁹⁰ and it is in remarkable agreement with the MD prediction (Figure 7).

The EnHD work set the stage for further design efforts. We have also investigated other members of the EnHD family. There is a change from 3-state to 2-state kinetics of folding across the homeodomain superfamily of proteins as the mechanism slides from framework to nucleation-condensation. The tendency for framework folding in this family correlates with inherent helical propensity. The cellular myeloblastis protein (c-Myb) falls in the mechanistic transition region. In-depth analysis of the MD trajectories showed that folding can be attributed to both of these mechanisms in different regions of the protein.¹⁸⁸ Experimentally, however, c-Myb folds by apparent two-state kinetics, but the MD simulations predict that the kinetics hide a high-energy intermediate.¹⁸⁸ The primary distinction between c-Myb and other members of the homeodomain family is that c-Myb has 5 (rather than 4) residues in the loop connecting the second and third helices. A mutant with a deletion of P174 was predicted to increase the helical propensity of helix 2 and to stabilize the turn connecting H2 and H3. In simulations, deletion of P174 allowed for the formation of native like contacts in the helix-turn-helix motif. The intermediate state was more populated in the mutant than in the WT simulations. Urea induced unfolding of c-Myb fit a two-state folding transition. Urea induced unfolding of c-Myb P174 deviated from a two-state folding transition. Additional urea induced unfolding of c-Myb P174/L155A showed evidence for the buildup of an intermediate during folding. We stabilized this folding intermediate discovered by MD by deleting a residue (P174) in the loop between its second and third helices, and the mutant intermediate is long-lived in simulations. Later equilibrium and kinetic experiments demonstrated that folding of the P174 mutant is indeed 3-state.¹⁹² Their results showed that MD simulations can identify intermediate states that may be 'invisible' to experimental techniques.

Tenascin C is found in the extracellular matrix and regulates cell-matrix interactions through the transduction of mechanical forces to biological signals. Application of a stretching force induces unfolding of the fibronectin type III domain of Tenascin-C (TNfn3), resulting in lengthening of Tenascin-C. Atomic force microscopy (AFM) and steered MD simulations^{193,194} showed that force-induced unfolding of TNfn3 results in a complex unfolding pathway with two highly populated intermediate states. One strategy for modulating the mechanical stability of proteins is to incorporate a bi-His metal chelation site

into the protein¹⁹⁵. Based on MD-derived forced-unfolding intermediates of TNfn3, Zhuang et al. engineered a bi-His metal chelation site into TNfn3 that allows the mechanical stability of Tenascin-C to be modulated, and it may be used to regulate the activity of ECM proteins in vivo¹⁹⁶. Two intermediate states are populated along the forced-unfolding trajectory, I₁ and I₂, and AFM suggested that the rate-limiting unfolding transition state lies between the intermediates. A hydrogen bond between the backbone atoms of residues 6 and 23 was associated with the transition from I₁ to I₂ in the simulations and a metal chelation site was incorporated to increase the energy barrier of the transition state for force-induced unfolding. Both chemical unfolding experiments and AFM showed increased TNfn3 stability in the presence of Ni²⁺, which coordinates with the designed bi-His residues. Thus, the mechanical stability of mutants that incorporate a designed chelation site can be tuned by the addition or removal of Ni²⁺. This approach may be extended to other protein where modulation of mechanical signal transduction is desired.

4.3 Probing misfolded states of proteins

Unfolding simulations, like those discussed above, can also be used to characterize vulnerabilities in structures associated with disease, such as the consequences of single nucleotide polymorphisms¹⁹⁷ and misfolding diseases. With respect to misfolding diseases, this is something of a misnomer. Instead of a competition between misfolding and folding correctly to the native state, these amyloidogenic proteins fold correctly but then partially unfold, often in response to low pH, and misfold into aggregation prone amyloidogenic intermediate states. The process of amyloidogenesis is characterized by the conversion of soluble, native conformations into toxic soluble oligomers and finally mature fibrils^{198,199}. There are now over 40 different human amyloid diseases²⁰⁰. Characterization of the conformational conversions during amyloidogenesis has not been possible using traditional structure determination methods due to dynamics, aggregation, and heterogeneity of the species. To this end, MD simulations can be applied to flesh out the molecular aspects of the process, typically triggering the process by lowering the pH.

In particular, as it was becoming clear that experimental methods were not able to provide detailed accounts of the conformational changes involved in amyloidogenesis, MD were employed in an effort to map the process. The first such account focused on the prion protein and the pH-induced changes in the structure in MD are in good agreement with experiment.^{201,202} Some altered β -sheet-like structure was observed in the resulting putative amyloidogenic intermediate states and more extensive simulations with other amyloidogenic proteins with diverse topologies showed that they, too, adopt α -sheet structure, including transthyretin^{203–206}, lysozyme²⁰⁷, β_2 -microglobulin²⁰⁸, and polyglutamine^{209,210}. Interestingly, α -sheet structure was modeled by Pauling and Corey in 1951,²¹¹ but they, rightly, dismissed it in favor of β -sheet structure for native folded proteins. α -sheets are similar to β -sheets except that instead of being formed by successive residues in the β -region of (ϕ , ψ) space, they alternate between α_L and α_R conformations, which produce an extended sheet with the main chain carbonyls aligned on one side of the strand and the amide NH groups on the other (Figure 8).

Based on the MD, we proposed the α -sheet hypothesis, which posits that α -sheet structure is shared by unrelated amyloidogenic proteins and is linked to toxicity and harbored by the toxic oligomers^{204,212}. As such, α -sheet structure represents a novel target for neutralizing toxicity and inhibiting fibril formation by employing the molecular dynamics-generated structures for rational structure-based design to create structurally complementary inhibitors (Figure 8). To this end, anti- α -sheet peptides, which are themselves α -sheets, were designed *in silico*, tested by MD and the highest-ranking designs were synthesized and tested experimentally. The designs make use of alternating D- and L-amino acids to help lock in the α -sheet structure, making use of conformational propensity^{125,213–215} and rotamer libraries^{216–218} for D- and L-amino acids from our Dymeomics project,^{219–220} which contains simulations of representatives of essentially all known protein folds and multiple host-guest peptide systems. This MD-derived Dymeomics database is another way in which MD can contribute to design efforts, as it contains 10⁵ more structures than the Protein Data Bank and represents a rich source of information regarding dynamic protein structures in solution.

If the α -sheet hypothesis is correct, then an α -sheet design should prevent aggregation in multiple amyloid systems. This is found to be the case, the designs α -sheet inhibitors preferentially bind the toxic oligomeric species and inhibit aggregation of A β (associated with Alzheimer's disease), transthyretin (systemic amyloid disease) and amylin (type 2 diabetes).^{123,124} Furthermore, all α -sheet designs investigated to date inhibit amyloidogenesis independent of sequence such that the stability of the α -sheet structure determines inhibitory potency not the sequence *per se*.¹²⁴ These inhibitors are unique in their mechanism of action through selective binding to the toxic oligomers, which supports the idea that the toxic species formed during amyloidogenesis adopt α -sheet and that unrelated amyloidogenic proteins and peptides funnel through this structure despite having different sequences and native structures. MD has been crucial to these design efforts, as without the MD the α -sheet structure would not have been discovered and this new family of cross-reacting amyloid inhibitors represent the only compounds that specifically target the toxic oligomeric species.

MD simulations have also been used to modulate the aggregation propensity of β_2 -microglobulin to form amyloid^{221,222}. In particular, Fogolari et al.²²² investigated the behavior of β_2 -microglobulin monomers under amyloidogenic conditions and suggested that W60 and other neighboring hydrophobic residues play a role in the early stages of aggregation by providing a hydrophobic interface for intermolecular association²²². Interestingly, this region formed α -sheet structure in the earlier simulations discussed above²⁰⁸, and Fogolari et al. also noted that D59/W60 formed the α -sheet repeating unit in their simulations. Mutation of W60 to Gly (W60G) resulted in a variant that is less prone to aggregation²²³. More recently, Camilloni et al. performed extensive replica averaged metadynamics simulations of WT and W60G β_2 -microglobulin to gain insights into the relationship between conformational flexibility and aggregation propensity. These simulations allowed for the design of variants with diverse aggregation kinetics²²¹.

5. Conclusions

Protein dynamics underlie mechanisms of protein stability, function, and folding. Because of this relationship, consideration of protein dynamics provides unique perspectives for protein design. Molecular dynamics simulations can provide critical insights into the relationship between protein dynamics and function, thereby leading to novel designs unobtainable through the use of static native structures alone. Furthermore, MD is unparalleled in its ability to provide atomic details of distinct nonnative conformational states as well as the transitions between these states that may be inaccessible by other techniques. Dynamics can be incorporated into different points in the protein design cycle. For example, simulations of wild type proteins performed prior to protein design can directly aid in the rational design of protein variants. After proteins have been designed, simulations can be used to evaluate and systematically rank them. A common strength of MD for protein design is to identify the optimal residues for making mutations. MD simulations can also help filter through candidate mutations derived from other computational design tools. Finally, there is a high degree of synergy between MD and other techniques: it can provide atomic details of mechanisms identified by experiment. In turn, experiment can confirm or reject predictions made by MD. As computational protein design matures, our understanding of the complex interplay between structure, dynamics, and function improves and as does our ability to use this information for applications in industry and medicine.

Acknowledgments

We are grateful for financial support provided by the National Institutes of Health (GMS 95808).

Biographies

Matthew Carter Childers: Matthew received his B.Sc. in Biomedical Engineering from the School of Engineering and Applied Science at the University of Virginia in 2013.

Afterwards, he began pursuing a Ph.D. in Bioengineering at the University of Washington under the mentorship of Dr. Valerie Daggett.

Valerie Daggett: Valerie Daggett received her Ph.D. in Pharmaceutical Chemistry from the University of California, San Francisco with Drs. Irwin Kuntz and Peter Kollman.

Afterwards, she completed a postdoctoral fellowship with Dr. Michael Levitt at Stanford University. She joined the faculty at the University of Washington in 1993 where she is a Professor of Bioengineering, Biochemistry, Chemical Engineering, and Biomedical and Health Informatics.

References

1. Gutte B. A synthetic 70-amino acid residue analog of ribonuclease S-protein with enzymic activity. *J. Biol. Chem.* 1975; 250:889–904. [PubMed: 1112795]
2. Gutte B. Study of RNase A mechanism and folding by means of synthetic 63-residue analogs. *J. Biol. Chem.* 1977; 252:663–670. [PubMed: 833149]
3. Levitt M, Greer J. Automatic identification of secondary structure in globular proteins. *J. Mol. Biol.* 1977; 114:181–239. [PubMed: 909086]

4. Kaiser ET, Kézdy FJ. Secondary structures of proteins and peptides in amphiphilic environments. *Proc. Natl. Acad. Sci. U. S. A.* 1983; 80:1137–1143. [PubMed: 6573659]
5. Moser R, et al. Expression of the synthetic gene of an artificial DDT-binding polypeptide in *Escherichia coli*. *Protein Eng. Des. Sel.* 1987; 1:339–343.
6. Moser R, Thomas RM, Gutte B. An artificial crystalline DDT-binding polypeptide. *FEBS Lett.* 1983; 157:247–251.
7. Gutte B, Däumigen M, Wittschieber E. Design, synthesis and characterisation of a 34-residue polypeptide that interacts with nucleic acids. *Nature.* 1979; 281:650–655. [PubMed: 551285]
8. Hecht M, Richardson J, Richardson D, Ogden R. De novo design, expression, and characterization of Felix: a four-helix bundle protein of native-like sequence. *Science.* 1990; 249:973. [PubMed: 2396098]
9. Erickson, B., et al. *Computer Graphics and Molecular Modeling*. Fletterick, R., Zoller, M., editors. Cold Spring Harbor Laboratory; 1986. p. 53-57.
10. Richardson JS, Richardson DC. The de novo design of protein structures. *Trends Biochem. Sci.* 1989; 14:304–309. [PubMed: 2672455]
11. Dunbrack RL, Karplus M. Backbone-dependent rotamer library for proteins. Application to side-chain prediction. *J. Mol. Biol.* 1993; 230:543–574. [PubMed: 8464064]
12. Wilson C, Gregoret LM, Agard DA. Modeling side-chain conformation for homologous proteins using an energy-based rotamer search. *J. Mol. Biol.* 1993; 229:996–1006. [PubMed: 8445659]
13. Dahiyat BI, Mayo SL. De novo protein design: fully automated sequence selection. *Science.* 1997; 278:82–87. [PubMed: 9311930]
14. Kuhlman B, et al. Design of a novel globular protein fold with atomic-level accuracy. *Science.* 2003; 302:1364–1368. [PubMed: 14631033]
15. Sterner R, Merkl R, Raushel FM. Computational Design of Enzymes. *Chem. Biol.* 2008; 15:421–423. [PubMed: 18482694]
16. Sivaramakrishnan S, Ashley E, Leinwand L, Spudich JA. Insights into human beta-cardiac myosin function from single molecule and single cell studies. *J. Cardiovasc. Transl. Res.* 2009; 2:426–440. [PubMed: 20560001]
17. Eisenmesser EZ, et al. Intrinsic dynamics of an enzyme underlies catalysis. *Nature.* 2005; 438:117–121. [PubMed: 16267559]
18. Eisenmesser EZ, Bosco DA, Akke M, Kern D. Enzyme dynamics during catalysis. *Science.* 2002; 295:1520–1523. [PubMed: 11859194]
19. Allen, MP, Tildesley, DJ. *Computer Simulations of Liquids*. Clarendon Press; 1987.
20. Palmer AG. NMR probes of molecular dynamics: Overview and comparison with other techniques. *Annu. Rev. Biophys. Biomol. Struct.* 2001; 30:129–155. [PubMed: 11340055]
21. van den Bedem H, Fraser JS. Integrative, dynamic structural biology at atomic resolution--it's about time. *Nat. Methods.* 2015; 12:307–318. [PubMed: 25825836]
22. Dror RO, Jensen MØ, Borhani DW, Shaw DE. Exploring atomic resolution physiology on a femtosecond to millisecond timescale using molecular dynamics simulations. *J. Gen. Physiol.* 2010; 135:555–562. [PubMed: 20513757]
23. Romo TD, Grossfield A. Unknown unknowns: the challenge of systematic and statistical error in molecular dynamics simulations. *Biophys J.* 2014; 106:1553–1554. [PubMed: 24739152]
24. Monticelli L, Tieleman DP. *Methods in Molecular Biology.* 2013; 924:197–213. [PubMed: 23034750]
25. Cino EA, Choy W-Y, Karttunen M. Comparison of Secondary Structure Formation Using 10 Different Force Fields in Microsecond Molecular Dynamics Simulations. *J. Chem. Theory Comput.* 2012; 8:2725–2740. [PubMed: 22904695]
26. Price DJ, Brooks CL. Modern protein force fields behave comparably in molecular dynamics simulations. *J Comput Chem.* 2002; 23:1045–1057. [PubMed: 12116391]
27. Lindorff-Larsen K, et al. Systematic validation of protein force fields against experimental data. *PLoS One.* 2012; 7:e32131. [PubMed: 22384157]

28. Beauchamp KA, Lin Y-S, Das R, Pande VS. Are Protein Force Fields Getting Better? A Systematic Benchmark on 524 Diverse NMR Measurements. *J. Chem. Theory Comput.* 2012; 8:1409–1414. [PubMed: 22754404]
29. Lange OF, van der Spoel D, de Groot BL. Scrutinizing molecular mechanics force fields on the submicrosecond timescale with NMR data. *Biophys J.* 2010; 99:647–655. [PubMed: 20643085]
30. Gu Y, Li D-WW, Brüschweiler R. NMR Order Parameter Determination from Long Molecular Dynamics Trajectories for Objective Comparison with Experiment. *J Chem Theory Comput.* 2014; 10:2599–2607. [PubMed: 26580780]
31. O'Brien ES, Wand AJ, Sharp KA. On the ability of molecular dynamics force fields to recapitulate NMR derived protein side chain order parameters. *Protein Sci.* 2016; 25:1156–1160. [PubMed: 26990788]
32. Beck DAC, Armen RS, Daggett V. Cutoff size need not strongly influence molecular dynamics results on solvated polypeptides. *Biochemistry.* 2005; 44:609–616. [PubMed: 15641786]
33. Hernández G, Anderson JS, Lemaster DM. Experimentally assessing molecular dynamics sampling of the protein native state conformational distribution. *Biophys. Chem.* 2012; 163–164:21–34.
34. Cunha KC, et al. Assessing protein conformational sampling and structural stability via de novo design and molecular dynamics simulations. *Biopolymers.* 2015; 103:351–361. [PubMed: 25677872]
35. Bond SD, Leimkuhler BJ. Molecular dynamics and the accuracy of numerically computed averages. *Acta Numer.* 2007; 16:1–65.
36. Rapaport, DCC. *The Art of Molecular Dynamics Simulation*. Second. Cambridge University Press; 2004.
37. Skeel RD. *The Graduate Student's Guide to Numerical Analysis '98*. 1999; 26:119–176.
38. Tuckerman ME, Martyna GJ. *Understanding Modern Molecular Dynamics: Techniques and Applications*. *J. Phys. Chem. B.* 2000; 104:159–178.
39. Levitt M, Hirshberg M, Sharon R, Laidig KE, Daggett V. Calibration and Testing of a Water Model for Simulation of the Molecular Dynamics of Proteins and Nucleic Acids in Solution. *J. Phys. Chem.* 1997; 101:5051–5061.
40. Shaw DE, et al. Atomic-level characterization of the structural dynamics of proteins. *Science.* 2010; 330:341–346. [PubMed: 20947758]
41. Lindorff-Larsen K, Maragakis P, Piana S, Shaw DE. Picosecond to Millisecond Structural Dynamics in Human Ubiquitin. *J. Phys. Chem. B.* 2016; 120:8313–8320. [PubMed: 27082121]
42. Abraham MJ, et al. GROMACS: High performance molecular simulations through multi-level parallelism from laptops to supercomputers. *SoftwareX.* 2015; 1:19–25.
43. Pande VS, et al. Atomistic protein folding simulations on the submillisecond time scale using worldwide distributed computing. *Biopolymers.* 2003; 68:91–109. [PubMed: 12579582]
44. van Gunsteren WF, Dolenc J, Mark AE. Molecular simulation as an aid to experimentalists. *Current Opinion in Structural Biology.* 2008; 18:149–153. [PubMed: 18280138]
45. van Gunsteren WF, Mark AE. Validation of molecular dynamics simulation. *J. Chem. Phys.* 1998; 108:6109.
46. Daggett V. Molecular Dynamics Simulations of the Protein Unfolding/Folding Reaction. *Acc. Chem. Res.* 2002; 35:422–429. [PubMed: 12069627]
47. Haki GD, Rakshit SK. Developments in industrially important thermostable enzymes: a review. *Bio. Technol.* 2003; 89:17–34.
48. Choi J-M, Han S-S, Kim H-S. Industrial applications of enzyme biocatalysis: Current status and future aspects. *Biotechnol. Adv.* 2015; 33:1443–1454. [PubMed: 25747291]
49. Wilson CJ. Rational protein design: developing next-generation biological therapeutics and nanobiotechnological tools. *WIREs Nanomed Nanobiotechnol.* 2015; 7:330–341.
50. Pace CN, Shirley BA, McNutt M, Gajiwala K. Forces contributing to the conformational stability of proteins. *FASEB J.* 1996; 10:75–83. [PubMed: 8566551]
51. Yokota A, Takahashi H, Takenawa T, Arai M. Probing the roles of conserved arginine-44 of *Escherichia coli* dihydrofolate reductase in its function and stability by systematic sequence

- perturbation analysis. *Biochem. Biophys. Res. Commun.* 2010; 391:1703–1707. [PubMed: 20043879]
52. Torrado M, et al. Role of conserved salt bridges in homeodomain stability and DNA binding. *J. Biol. Chem.* 2009; 284:23765–23779. [PubMed: 19561080]
53. Jomain J-B, et al. Structural and thermodynamic bases for the design of pure prolactin receptor antagonists: X-ray structure of Del1-9-G129R-hPRL. *J. Biol. Chem.* 2007; 282:33118–33131. [PubMed: 17785459]
54. Fredricksen RS, Swenson CA. Relationship between stability and function for isolated domains of troponin C. *Biochemistry.* 1996; 35:14012–14026. [PubMed: 8909299]
55. Stouffer AL, Nanda V, Lear JD, DeGrado WF. Sequence determinants of a transmembrane proton channel: an inverse relationship between stability and function. *J. Mol. Biol.* 2005; 347:169–179. [PubMed: 15733926]
56. Masazumi M, Signor G, Matthews BW. Substantial increase of protein stability by multiple disulphide bonds. *Nature.* 1989; 342:291–293. [PubMed: 2812028]
57. Sikosek T, Chan HS. Biophysics of protein evolution and evolutionary protein biophysics. *J. Roy. Soc. Interface.* 2014; 11:20140419. [PubMed: 25165599]
58. Kapoor S, Rafiq A, Sharma S. Protein Engineering and Its Applications in Food Industry. *Crit. Rev. Food Sci. Nutr.* 2015; 11:0.
59. Teilum K, Olsen JG, Kragelund BB. Protein stability, flexibility and function. *Biochim. Biophys. Acta (BBA)-Proteins Proteomics.* 2011; 1814:969–976. [PubMed: 21094283]
60. Clarke J, Hounslow AM, Bond CJ, Fersht AR, Daggett V. The effects of disulfide bonds on the denatured state of barnase. *Protein Sci.* 2000; 9:2394–2404. [PubMed: 11206061]
61. Pendley SS, Yu YB, Cheatham TE. Molecular dynamics guided study of salt bridge length dependence in both fluorinated and non-fluorinated parallel dimeric coiled-coils. *Proteins.* 2009; 74:612–629. [PubMed: 18704948]
62. Chao S-HH, et al. Two structural scenarios for protein stabilization by PEG. *J Phys Chem B.* 2014; 118:8388–8395. [PubMed: 24821319]
63. Xiao S, et al. Rational modification of protein stability by targeting surface sites leads to complicated results. *Proc Natl Acad Sci U S A.* 2013; 110:11337–11342. [PubMed: 23798426]
64. Berman HM1, Westbrook J, Feng Z, Gilliland G, Bhat TN, Weissig H, Shindyalov IN, Bourne PE. The Protein Data Bank. *Nucleic Acids Res.* 2000; 28:235–242. [PubMed: 10592235]
65. Flory PJ. Statistical Thermodynamics of Semi-Flexible Chain Molecules. *Proc. R. Soc. A Math. Phys. Eng. Sci.* 1956; 234:60–73.
66. Doig AJ, Williams DH. Is the hydrophobic effect stabilizing or destabilizing in proteins?: The contribution of disulphide bonds to protein stability. *J. Mol. Biol.* 1991; 217:389–398. [PubMed: 1992169]
67. Clarke J, Fersht AR. Engineered disulfide bonds as probes of the folding pathway of barnase: increasing the stability of proteins against the rate of denaturation. *Biochemistry.* 1993; 32:4322–4329. [PubMed: 8476861]
68. Johnson CM, Oliveberg M, Clarke J, Fersht AR. Thermodynamics of denaturation of mutants of barnase with disulfide crosslinks. *J. Mol. Biol.* 1997; 268:198–208. [PubMed: 9149152]
69. Betz SF. Disulfide bonds and the stability of globular proteins. *Protein Sci.* 1993; 2:1551–1558. [PubMed: 8251931]
70. Pikkemaat MG, Linssen ABM, Berendsen HJC, Janssen DB. Molecular dynamics simulations as a tool for improving protein stability. *Protein Eng.* 2002; 15:185–192. [PubMed: 11932489]
71. Hazes B, Dijkstra BW. Model building of disulfide bonds in proteins with known three-dimensional structure. *Protein Eng.* 1988; 2:119–125. [PubMed: 3244694]
72. Niu C, Zhu L, Xu X, Li Q. Rational Design of Disulfide Bonds Increases Thermostability of a Mesophilic 1,3-1,4- β -Glucanase from *Bacillus terquilensis*. *PLoS One.* 2016; 11:e0154036. [PubMed: 27100881]
73. Yu H, Huang H. Engineering proteins for thermostability through rigidifying flexible sites. *Biotechnology Advances.* 2014; 32:308–315. [PubMed: 24211474]

74. Daggett V, Levitt M. A model of the molten globule state from molecular dynamics simulations. *Proc. Natl. Acad. Sci. U. S. A.* 1992; 89:5142–5146. [PubMed: 1594623]
75. Daggett V, Levitt M. Protein unfolding pathways explored through molecular dynamics simulations. *J Mol Biol.* 1993; 232:600–619. [PubMed: 7688428]
76. Levitt M, Hirshberg M, Sharon R, Daggett V. Potential Energy Function and Parameters for Simulations of the Molecular Dynamics of Proteins and Nucleic Acids in Solution. *Computer Physics Commun.* 1995; 91:215–231.
77. Matouschek A1, Kellis JT Jr, Serrano L, Fersht AR. Mapping the transition state and pathway of protein folding by protein engineering. *Nature.* 1989; 340:122–126. [PubMed: 2739734]
78. Daggett V, Li A, Itzhaki LS, Otzen DE, Fersht AR. Structure of the transition state for folding of a protein derived from experiment and simulation. *J. Mol. Biol.* 1996; 257:430–440. [PubMed: 8609634]
79. Kulkarni N, Shendye A, Rao M. Molecular and biotechnological aspects of xylanases. *FEMS Microbiol. Rev.* 1999; 23:411–456. [PubMed: 10422261]
80. Beg Q, Kapoor M, Mahajan L, Hoondal GS. Microbial xylanases and their industrial applications: a review. *Appl. Microbiol. Biotechnol.* 2001; 56:326–338. [PubMed: 11548999]
81. Collins T, Gerday C, Feller G. Xylanases, xylanase families and extremophilic xylanases. *FEMS Microbiol Rev.* 2005; 29:3–23. [PubMed: 15652973]
82. Joo JC, Pohkrel S, Pack SP, Yoo YJ. Thermostabilization of *Bacillus circulans* xylanase via computational design of a flexible surface cavity. *J. Biotechnol.* 2010; 146:31–39. [PubMed: 20074594]
83. Wells S, Menor S, Hespeneide B, Thorpe MF. Constrained geometric simulation of diffusive motion in proteins. *Phys Biol.* 2005; 2:S127–S136. [PubMed: 16280618]
84. Joo JC, Pack SP, Kim YH, Yoo YJ. Thermostabilization of *Bacillus circulans* xylanase: Computational optimization of unstable residues based on thermal fluctuation analysis. *J. Biotechnol.* 2011; 151:56–65. [PubMed: 20959126]
85. Liu Y, Kuhlman B. RosettaDesign server for protein design. *Nucleic Acids Res.* 2006; 34:W235–W238. [PubMed: 16845000]
86. Vogt G, Woell S, Argos P. Protein thermal stability, hydrogen bonds, and ion pairs. *J. Mol. Biol.* 1997; 269:631–643. [PubMed: 9217266]
87. Merkley ED, Parson WW, Daggett V. Temperature dependence of the flexibility of thermophilic and mesophilic flavoenzymes of the nitroreductase fold. *Protein Eng. Des. Sel.* 2010; 23:327–336. [PubMed: 20083491]
88. Szilágyi A, Závodszy P. Structural differences between mesophilic, moderately thermophilic and extremely thermophilic protein subunits: results of a comprehensive survey. *Structure.* 2000; 8:493–504. [PubMed: 10801491]
89. Yokota K, Satou K, Ohki S-Y. Comparative analysis of protein thermostability: differences in amino acid content and substitution at the surfaces and in the core regions of thermophilic and mesophilic proteins. *Sci. Technol. Adv. Mater.* 2006; 7:255–262.
90. Vieira DS, Degreve L. An insight into the thermostability of a pair of xylanases: the role of hydrogen bonds. *Mol. Phys.* 2009; 107:59–69.
91. Vieira DS, Degrève L, Ward RJ. Characterization of temperature dependent and substrate-binding cleft movements in *Bacillus circulans* family 11 xylanase: a molecular dynamics investigation. *Biochim Biophys Acta.* 2009; 1790:1301–1306. [PubMed: 19409448]
92. Alpointi JS, Fonseca Maldonado R, Ward RJ. Thermostabilization of *Bacillus subtilis* GH11 xylanase by surface charge engineering. *Int J Biol Macromol.* 2016; 87:522–528. [PubMed: 26955749]
93. Chen J, Yu H, Liu C, Liu J, Shen Z. Improving stability of nitrile hydratase by bridging the salt-bridges in specific thermal-sensitive regions. *J Biotechnol.* 2012; 164:354–362. [PubMed: 23384947]
94. Li J, Mahajan A, Tsai MD. Ankyrin repeat: A unique motif mediating protein-protein interactions. *Biochemistry.* 2006; 45:15168–15178. [PubMed: 17176038]
95. Mosavi LK, Cammett TJ, Desrosiers DC, Peng Z-Y. The ankyrin repeat as molecular architecture for protein recognition. *Protein Sci.* 2004; 13:1435–1448. [PubMed: 15152081]

96. Porebski BT, Buckle AM. Consensus protein design. *Protein Eng. Des. Sel.* 2016; 29:245–251. [PubMed: 27274091]
97. Binz HK, Stumpp MT, Forrer P, Amstutz P, Plückthun A. Designing repeat proteins: Well-expressed, soluble and stable proteins from combinatorial libraries of consensus ankyrin repeat proteins. *J. Mol. Biol.* 2003; 332:489–503. [PubMed: 12948497]
98. Forrer P, Stumpp MT, Binz HK, Plückthun A. A novel strategy to design binding molecules harnessing the modular nature of repeat proteins. *FEBS Letters.* 2003; 539:2–6. [PubMed: 12650916]
99. Interlandi G, Wetzel SK, Settanni G, Plückthun A, Cafilisch A. Characterization and further stabilization of designed ankyrin repeat proteins by combining molecular dynamics simulations and experiments. *J. Mol. Biol.* 2008; 375:837–854. [PubMed: 18048057]
100. Alfarano P, et al. Optimization of designed armadillo repeat proteins by molecular dynamics simulations and NMR spectroscopy. *Protein Sci.* 2012; 21:1298–1314. [PubMed: 22767482]
101. Yang A-S, Honig B. On the pH Dependence of Protein Stability. *J. Mol. Biol.* 1993; 231:459–474. [PubMed: 8510157]
102. Oinonen C, Rouvinen J. Structural comparison of Ntn-hydrolases. *Protein Sci.* 2000; 9:2329–2337. [PubMed: 11206054]
103. Arroyo M, de la Mata I, Acebal C, Castellón MP. Biotechnological applications of penicillin acylases: state-of-the-art. *Appl. Microbiol. Biotechnol.* 2003; 60:507–514. [PubMed: 12536249]
104. Guranda DT, Volovik TS, Svedas VK. pH Stability of penicillin acylase from *Escherichia coli*. *Biochem. Biokhimii.* 2004; 69:1386–1390.
105. Suplatov D, et al. Computational design of a pH stable enzyme: understanding molecular mechanism of penicillin acylase's adaptation to alkaline conditions. 2014
106. Leone S, et al. Molecular Dynamics Driven Design of pH-Stabilized Mutants of MNEI, a Sweet Protein. *PLoS One.* 2016; 11:e0158372. [PubMed: 27340829]
107. Strumillo M, Beltrao P. Towards the computational design of protein post-translational regulation. *Bioorg. Med. Chem.* 2015; 23:2877–2882. [PubMed: 25956846]
108. Huang K-Y. dbPTM 2016: 10-year anniversary of a resource for post-translational modification of proteins. *Nucleic Acids Res.* 2016; 44:D435–D446. [PubMed: 26578568]
109. Khoury GA, et al. Proteome-wide post-translational modification statistics: frequency analysis and curation of the swiss-prot database. *Sci. Rep.* 2011; 1:4–8. [PubMed: 22355523]
110. Solá RJ, Griebenow K. Effects of glycosylation on the stability of protein pharmaceuticals. *J. Pharm. Sci.* 2009; 98:1223–1245. [PubMed: 18661536]
111. Apweiler R, Hermjakob H, Sharon N. On the frequency of protein glycosylation, as deduced from analysis of the SWISS-PROT database. *Biochim. Biophys. Acta.* 1999; 1473:4–8. [PubMed: 10580125]
112. Sinclair AM, Elliott S. Glycoengineering: The effect of glycosylation on the properties of therapeutic proteins. *J. Pharm. Sci.* 2005; 94:1626–1635. [PubMed: 15959882]
113. Baker JL, Çelik E, DeLisa MP. Expanding the glycoengineering toolbox: the rise of bacterial N-linked protein glycosylation. *Trends Biotechnol.* 2013; 31:313–323. [PubMed: 23582719]
114. Hellinga HW. Rational protein design: combining theory and experiment. *Proc. Natl. Acad. Sci. U. S. A.* 1997; 94:10015–10017. [PubMed: 9294154]
115. Berezovsky IN, Zeldovich KB, Shakhnovich EI. Positive and negative design in stability and thermal adaptation of natural proteins. *PLoS Comput. Biol.* 2007; 3:e52. [PubMed: 17381236]
116. Samoudi M, et al. Rational design of hyper-glycosylated interferon beta analogs: A computational strategy for glycoengineering. *J. Mol. Graph. Model.* 2015; 56:31–42. [PubMed: 25544388]
117. Davey JA, Damry AM, Euler CK, Goto NK, Chica RA. Prediction of Stable Globular Proteins Using Negative Design with Non-native Backbone Ensembles. *Structure.* 2015; 23:2011–2021. [PubMed: 26412333]
118. Fonseca-Maldonado R, et al. Engineering the pattern of protein glycosylation modulates the thermostability of a GH11 xylanase. *J. Biol. Chem.* 2013; 288:25522–25534. [PubMed: 23846692]

119. Ramachandran GN, Ramakrishnan C, Sasisekharan V. Stereochemistry of polypeptide chain configurations. *J. Mol. Biol.* 1963; 7:95–99. [PubMed: 13990617]
120. Towse C-LC-L, Hopping G, Vulovic I, Daggett V. Nature versus design: the conformational propensities of D-amino acids and the importance of side chain chirality. *Protein Eng. Des. Sel.* 2014; 27:447–455. [PubMed: 25233851]
121. Rodriguez-Granillo A, Annavarapu S, Zhang L, Koder RL, Nanda V. Computational design of thermostabilizing D-amino acid substitutions. *J. Am. Chem. Soc.* 2011; 133:18750–18759. [PubMed: 21978298]
122. Imperiali B, Moats RA, Fisher SL, Prins TJ. A conformational study of peptides with the general structure Ac-L-Xaa-Pro-D-Xaa-L-Xaa-NH₂: spectroscopic evidence for a peptide with significant beta-turn character in water and in dimethyl sulfoxide. *J. Am. Chem. Soc.* 1992; 114:3182–3188.
123. Hopping G, et al. Designed α -sheet peptides inhibit amyloid formation by targeting toxic oligomers. *Elife.* 2014; 3:e01681. [PubMed: 25027691]
124. Kellock J, Hopping G, Caughey B, Daggett V. Peptides Composed of Alternating L- and D-Amino Acids Inhibit Amyloidogenesis in Three Distinct Amyloid Systems Independent of Sequence. *J. Mol. Biol.* 2016; 428:2317–2328. [PubMed: 27012425]
125. Rana S, Kundu B, Durani S. Stereospecific peptide folds. A rationally designed molecular bracelet. *Chem. Commun.* 2004:2462–2463.
126. Rana S, Kundu B, Durani S. A small peptide stereochemically customized as a globular fold with a molecular cleft. *Chem. Commun.* 2005:207–209.
127. Valiyaveetil FI, Sekedat M, Mackinnon R, Muir TW. Glycine as a D-amino acid surrogate in the K(+)-selectivity filter. *Proc. Natl. Acad. Sci. U. S. A.* 2004; 101:17045–17049. [PubMed: 15563591]
128. Makwana KM, Mahalakshmi R. Capping β -hairpin with N-terminal d-amino acid stabilizes peptide scaffold. *Biopolymers.* 2016; 106:260–266. [PubMed: 26999275]
129. Anderson EM, Larsson KM, Kirk O. One biocatalyst--many applications: the use of *Candida antarctica* B-lipase in organic synthesis. *Biocatal. Biotransformation.* 1998; 16:181–204.
130. Park HJ, Park K, Kim YH, Yoo YJ. Computational approach for designing thermostable *Candida antarctica* lipase B by molecular dynamics simulation. *J Biotechnol.* 2014; 192(Pt A):66–70. [PubMed: 25270022]
131. de la Mata I, et al. The impact of R53C mutation on the three-dimensional structure, stability, and DNA-binding properties of the human *Hesx-1* homeodomain. *ChemBiochem.* 2002; 3:726–740. [PubMed: 12203971]
132. Kinet S, Bernichtein S, Kelly PA, Martial JA, Goffin V. Biological properties of human prolactin analogs depend not only on global hormone affinity, but also on the relative affinities of both receptor binding sites. *J. Biol. Chem.* 1999; 274:26033–26043. [PubMed: 10473550]
133. Zakrzewska M, Krowarsch D, Wiedlocha A, Olsnes S, Otlewski J. Highly stable mutants of human fibroblast growth factor-1 exhibit prolonged biological action. *J. Mol. Biol.* 2005; 352:860–875. [PubMed: 16126225]
134. Julenius K, Thulin E, Linse S, Finn BE. Hydrophobic core substitutions in calbindin D9k: effects on stability and structure. *Biochemistry.* 1998; 37:8915–8925. [PubMed: 9636033]
135. Kragelund BB, et al. Hydrophobic core substitutions in calbindin D9k: effects on Ca²⁺ binding and dissociation. *Biochemistry.* 1998; 37:8926–8937. [PubMed: 9636034]
136. Morin A, Meiler J, Mizoue LS. Computational design of protein-ligand interfaces: potential in therapeutic development. *Trends Biotechnol.* 2011; 29:159–166. [PubMed: 21295366]
137. Liang S, et al. Exploring the molecular design of protein interaction sites with molecular dynamics simulations and free energy calculations. *Biochemistry.* 2009; 48:399–414. [PubMed: 19113835]
138. Janssen BJC, Halff EF, Lambris JD, Gros P. Structure of compstatin in complex with complement component C3c reveals a new mechanism of complement inhibition. *J. Biol. Chem.* 2007; 282:29241–29247. [PubMed: 17684013]
139. Ricklin D, Lambris JD. Compstatin: a complement inhibitor on its way to clinical application. *Adv. Exp. Med. Biol.* 2008; 632:273–292. [PubMed: 19025129]

140. Sahu A, Morikis D, Lambris JD. Compstatin, a peptide inhibitor of complement, exhibits species-specific binding to complement component C3. *Mol. Immunol.* 2003; 39:557–566. [PubMed: 12431389]
141. Tamamis P, et al. Design of a modified mouse protein with ligand binding properties of its human analog by molecular dynamics simulations: The case of C3 inhibition by compstatin. *Proteins Struct. Funct. Bioinforma.* 2011; 79:3166–3179.
142. Tamamis P, Morikis D, Floudas CA, Archontis G. Species specificity of the complement inhibitor compstatin investigated by all-atom molecular dynamics simulations. *Proteins Struct. Funct. Bioinforma.* 2010; 78:2655–2667.
143. Tamamis P, et al. Molecular Dynamics in Drug Design: New Generations of Compstatin Analogs. *Chem. Biol. Drug Des.* 2012; 79:703–718. [PubMed: 22233517]
144. Storch EM, Daggett V. Molecular dynamics simulation of cytochrome b₅: implications for protein-protein recognition. *Biochemistry.* 1995; 34:9682–9693. [PubMed: 7626638]
145. Moulton J. Comparison of database potentials and molecular mechanics force fields. *Curr. Opin. Struct. Biol.* 1997; 7:194–199. [PubMed: 9094335]
146. Storch EM, Daggett V, Atkins WM. Engineering out motion: introduction of a de novo disulfide bond and a salt bridge designed to close a dynamic cleft on the surface of cytochrome b₅. *Biochemistry.* 1999; 38:5054–5064. [PubMed: 10213608]
147. Storch EM, Grinstead JS, Campbell AP, Daggett V, Atkins WM. Engineering Out Motion: A Surface Disulfide Bond Alters the Mobility of Trp 22 in Cytochrome b₅ as Probed by Time-Resolved Fluorescence and ¹H-NMR Experiments. *Biochemistry.* 1999; 38:5065–5075. [PubMed: 10213609]
148. Michielssens S, et al. A designed conformational shift to control protein binding specificity. *Angew Chem Int Ed Engl.* 2014; 53:10367–10371. [PubMed: 25115701]
149. Dodani SC, et al. Structural, functional, and spectroscopic characterization of the substrate scope of the novel nitrating cytochrome P450 TxtE. *Chembiochem.* 2014; 15:2259–2267. [PubMed: 25182183]
150. Dodani SC, et al. Discovery of a regioselectivity switch in nitrating P450s guided by molecular dynamics simulations and Markov models. *Nat Chem.* 2016; 8:419–425. [PubMed: 27102675]
151. Beck DAC, Daggett V. A one-dimensional reaction-coordinate for identification of transition states from explicit solvent P_{fold}-like calculations. *Biophys. J.* 2007; 93:3382–3391. [PubMed: 17978165]
152. Kemp DS, Casey ML. Physical Organic Chemistry of Benzisoxazoles. II. Linearity of the Brønsted Free Energy Relationship for the Base-Catalyzed Decomposition of Benzisoxazoles.
153. Röthlisberger D, et al. Kemp elimination catalysts by computational enzyme design. *Nature.* 2008; 453:190–195. [PubMed: 18354394]
154. Thorn SN, Daniels RG, Auditor MT, Hilvert D. Large rate accelerations in antibody catalysis by strategic use of haptenic charge. *Nature.* 1995; 373:228–230. [PubMed: 7816136]
155. Hollfelder F, Kirby AJ, Tawfik DS. Off-the-shelf proteins that rival tailor-made antibodies as catalysts. *Nature.* 1996; 383:60–62. [PubMed: 8779715]
156. Korendovych IV, et al. Design of a switchable eliminase. *Proc. Natl. Acad. Sci. U. S. A.* 2011; 108:6823–6827. [PubMed: 21482808]
157. Zanghellini A, et al. New algorithms and an in silico benchmark for computational enzyme design. *Protein Sci.* 2006; 15:2785–2794. [PubMed: 17132862]
158. Privett HK, et al. Iterative approach to computational enzyme design. *Proc. Natl. Acad. Sci.* 2012; 109:3790–3795. [PubMed: 22357762]
159. Debler EW, et al. Structural origins of efficient proton abstraction from carbon by a catalytic antibody. *Proc. Natl. Acad. Sci. U. S. A.* 2005; 102:4984–4989. [PubMed: 15788533]
160. Jiang L, et al. De novo computational design of retro-aldol enzymes. *Science.* 2008; 319:1387–1391. [PubMed: 18323453]
161. List B, Barbas CF, Lerner RA. Aldol sensors for the rapid generation of tunable fluorescence by antibody catalysis. *Proc. Natl. Acad. Sci.* 1998; 95:15351–15355. [PubMed: 9860972]

162. Ruscio JZ, Kohn JE, Ball KA, Head-Gordon T. The influence of protein dynamics on the success of computational enzyme design. *J. Am Chem Soc.* 2009; 131:14111–14115. [PubMed: 19788332]
163. Wang L, et al. Structural analyses of covalent enzyme-substrate analog complexes reveal strengths and limitations of de novo enzyme design. *J. Mol. Biol.* 2012; 415:615–625. [PubMed: 22075445]
164. Kiss G, Pande VS, Houk KN. Molecular dynamics simulations for the ranking, evaluation, and refinement of computationally designed proteins. *Methods Enzymol.* 2013; 523:145–170. [PubMed: 23422429]
165. Kiss G, Röthlisberger D, Baker D, Houk KN. Evaluation and ranking of enzyme designs. *Protein Sci.* 2010; 19:1760–1773. [PubMed: 20665693]
166. Bjelic S, et al. Computational design of enone-binding proteins with catalytic activity for the Morita-Baylis-Hillman reaction. *ACS Chem. Biol.* 2013; 8:749–757. [PubMed: 23330600]
167. Alexander PA, Rozak DA, Orban J, Bryan PN. Directed Evolution of Highly Homologous Proteins with Different Folds by Phage Display: Implications for the Protein Folding Code. *Biochemistry.* 2005; 44:14045–14054. [PubMed: 16245920]
168. He Y, Yeh DC, Alexander P, Bryan PN, Orban J. Solution NMR structures of IgG binding domains with artificially evolved high levels of sequence identity but different folds. *Biochemistry.* 2005; 44:14055–14061. [PubMed: 16245921]
169. Scott KA, Daggett V. Folding mechanisms of proteins with high sequence identity but different folds. *Biochem.* 2007; 46:1545–1556. [PubMed: 17279619]
170. Morrone A, McCully ME, Bryan PN, Brunori M, Gianni S, Daggett V, Travaglini-Allocatelli C. The denatured state dictates the topology of two proteins with almost identical sequence but different native structure and function. *J. Biol. Chem.* 2011; 286:3863–3872. [PubMed: 21118804]
171. Day R, Daggett V. Direct observation of microscopic reversibility in protein folding. *J. Mol. Biol.* 2007; 366:677–686. [PubMed: 17174331]
172. McCully ME, Beck DAC, Daggett V. Microscopic reversibility of protein folding in molecular dynamics simulations of the engrailed homeodomain. *Biochemistry.* 2008; 47:4079–7089.
173. Li A, Daggett V. Characterization of the transition state of protein unfolding by use of molecular dynamics: chymotrypsin inhibitor 2. *Proc. Natl. Acad. Sci.* 1994; 91:10430–10434. [PubMed: 7937969]
174. Li A, Daggett V. Identification and characterization of the unfolding transition state of chymotrypsin inhibitor 2 by molecular dynamics simulations. *J. Mol. Biol.* 1996; 257:412–429. [PubMed: 8609633]
175. Ladurner AG, Itzhaki LS, Daggett V, Fersht AR. Synergy between simulation and experiment in describing the energy landscape of protein folding. *Proc. Natl. Acad. Sci. U. S. A.* 1998; 95:8473–8478. [PubMed: 9671702]
176. Levitt M. Molecular dynamics of native protein. II. Analysis and nature of motion. *J. Mol. Biol.* 1983; 168:621–657. [PubMed: 6193282]
177. Piana S, et al. Computational design and experimental testing of the fastest-folding β -sheet protein. *J Mol Biol.* 2011; 405:43–48. [PubMed: 20974152]
178. Cocco MJ, Lecomte JT. Characterization of hydrophobic cores in apomyoglobin: a proton NMR spectroscopy study. *Biochemistry.* 1990; 29:11067–11072. [PubMed: 2176892]
179. Jennings PA, Wright PE. Formation of a molten globule intermediate early in the kinetic folding pathway of apomyoglobin. *Science.* 1993; 262:892–896. [PubMed: 8235610]
180. Ballew RM, Sabelko J, Gruebele M. Direct observation of fast protein folding: the initial collapse of apomyoglobin. *Proc. Natl. Acad. Sci. U. S. A.* 1996; 93:5759–5764. [PubMed: 8650166]
181. Ballew RM, Sabelko J, Gruebele M. Observation of distinct nanosecond and microsecond protein folding events. *Nat Struct. Biol.* 1996; 3:923–926. [PubMed: 8901868]
182. Goodman JS, Chao SH, Pogorelov TV, Gruebele M. Filling up the heme pocket stabilizes apomyoglobin and speeds up its folding. *J. Phys. Chem. B.* 2014; 118:6511–6518. [PubMed: 24456280]

183. Garcia C, Nishimura C, Cavagnero S, Dyson HJ, Wright PE. Changes in the apomyoglobin folding pathway caused by mutation of the distal histidine residue. *Biochemistry*. 2000; 39:11227–11237. [PubMed: 10985768]
184. Picotti P, et al. Modulation of the structural integrity of helix F in apomyoglobin by single amino acid replacements. *Protein Sci*. 2004; 13:1572–1585. [PubMed: 15152090]
185. Mayor U, Johnson CM, Grossmann JG, Sato S, Jas GS, Freund SMV, Guydosh NR, Alonso DOV, Daggett V, Fersht AR. The Complete Folding Pathway of a Protein from Nanoseconds to Microseconds. *Nature*. 2003; 421:863–867. [PubMed: 12594518]
186. Mayor U, Johnson CM, Daggett V, Fersht AR. Protein folding and unfolding in microseconds to nanoseconds by experiment and simulation. *Proc. Natl. Acad. Sci USA*. 2000; 97:13518–13522. [PubMed: 11087839]
187. DeMarco ML, Alonso DOV, Daggett V. Diffusing and colliding: The atomic level folding/unfolding pathway of a small helical protein. *J. Mol. Biol*. 2004; 341:1109–1124. [PubMed: 15328620]
188. Gianni S, Guydosh NR, Khan F, Caldas TD, Mayor U, White GWN, DeMarco ML, Daggett V, Fersht AR. Unifying features in protein-folding mechanisms. 2003; 100:13286–13291.
189. McCully M, Beck DAC, Daggett V. Microscopic reversibility in single-molecule folding/unfolding of a protein at its T_m . *Biochemistry*. 2008; 47:7079–7089. [PubMed: 18553935]
190. Sharpe TD, Jonsson AL, Rutherford TJ, Daggett V, Fersht AR. The role of the turn in β -hairpin formation during WW domain folding. *Prot. Sci*. 2007; 16:2233–2239.
191. Religa TL, Markson JS, Mayor U, Freund SMV, Fersht AR. Solution structure of a protein denatured state and folding intermediate. *Nature*. 2005; 437:1053–1056. [PubMed: 16222301]
192. White GWN, Gianni S, Grossman JG, Jemth P, Fersht AR, Daggett V. Simulation and Experiment Conspire to reveal Cryptic Intermediates and the Slide from the Nucleation-Condensation to Framework Mechanism of Folding. *J. Mol. Biol*. 2005; 350:757–775. [PubMed: 15967458]
193. Peng Q, et al. Mechanical design of the third FnIII domain of tenascin-C. *J. Mol. Biol*. 2009; 386:1327–1342. [PubMed: 19452631]
194. Ng SP, et al. Mechanical unfolding of TNfn3: the unfolding pathway of a fnIII domain probed by protein engineering, AFM and MD simulation. *J. Mol. Biol*. 2005; 350:776–789. [PubMed: 15964016]
195. Cao Y, Yoo T, Li H. Single molecule force spectroscopy reveals engineered metal chelation is a general approach to enhance mechanical stability of proteins. *Proc. Natl. Acad. Sci. U. S. A*. 2008; 105:11152–11157. [PubMed: 18685107]
196. Zhuang S, Peng Q, Cao Y, Li H. Modulating the Mechanical Stability of Extracellular Matrix Protein Tenascin-C in a Controlled and Reversible Fashion. *J. Mol. Biol*. 2009; 390:820–829. [PubMed: 19477181]
197. Rutherford K, Daggett V. Polymorphisms and Disease: Hotspots of Inactivation in Methyltransferases. *Trends in Biochem. Sci*. 2010; 35:531–538. [PubMed: 20382027]
198. Chiti F, Dobson CM. Protein misfolding, functional amyloid, and human disease. *Annu. Rev Biochem*. 2006; 75:333–366. [PubMed: 16756495]
199. Haass C, Selkoe DJ. Soluble protein oligomers in neurodegeneration: lessons from the Alzheimer's amyloid beta-peptide. *Nat. Rev. Mol. Cell Biol*. 2007; 8:101–112. [PubMed: 17245412]
200. Sipe JD, et al. Nomenclature 2014: Amyloid fibril proteins and clinical classification of the amyloidosis. *Amyloid*. 2014; 21:221–224. [PubMed: 25263598]
201. Alonso DOV, DeArmond S, Cohen F, Daggett V. Mapping the Early Steps in the Conversion of the Prion Protein. *Proc. Natl. Acad. Sci. USA*. 2001; 98:2985–2989. [PubMed: 11248018]
202. Alonso DOV, An C, Daggett V. Simulations of Biomolecules: Characterization of the Early Steps in the pH-Induced Conformational Conversion of the Hamster, Bovine, and Human Forms of the Prion Protein. *Phil. Tran. Roy. Soc*. 2002; 360:1165–1178.
203. Armen RS, Alonso DOV, Daggett V. Anatomy of an amyloidogenic intermediate: Conversion of β -sheet to α -sheet structure in transthyretin at acidic pH. *Structure*. 2004; 12:1847–1863. [PubMed: 15458633]

204. Armen RS, DeMarco ML, Alonso DOV, Daggett V. Pauling and Corey's alpha-pleated sheet structure may define the prefibrillar amyloidogenic intermediate in amyloid disease. *Proc. Natl. Acad. Sci. U. S. A.* 2004; 101:11622–11627. [PubMed: 15280548]
205. Steward RE, Armen RS, Daggett V. Different disease-causing mutations in transthyretin trigger the same conformational conversion. *Protein Eng. Des. Sel.* 2008; 21:187–195. [PubMed: 18276611]
206. Yang M, Lei M, Yordanov B, Huo S. Peptide plane can flip in two opposite directions: Implication in amyloid formation of transthyretin. *J. Phys. Chem. B.* 2006; 110:5829–5833. [PubMed: 16553385]
207. Kazmirski SL, Daggett V. Non-native interactions in protein folding intermediates: molecular dynamics simulations of hen lysozyme. *J. Mol. Biol.* 1998; 284:793–806. [PubMed: 9826516]
208. Armen RS, Daggett V. Characterization of two distinct beta2-microglobulin unfolding intermediates that may lead to amyloid fibrils of different morphology. *Biochemistry.* 2005; 44:16098–16107. [PubMed: 16331970]
209. Armen RS, Bernard BM, Day R, Alonso DOV, Daggett V. Characterization of a possible amyloidogenic precursor in glutamine-repeat neurodegenerative diseases. *Proc. Natl. Acad. Sci. U. S. A.* 2005; 102:13433–13438. [PubMed: 16157882]
210. Babin V, Roland C, Sagui C. The α -sheet: A missing-in-action secondary structure? *Proteins.* 2011; 79:937–946. [PubMed: 21287624]
211. Pauling L, Corey RB. The pleated sheet, a new layer configuration of polypeptide chains. *Proc. Natl. Acad. Sci. U. S. A.* 1951; 37:251–256. [PubMed: 14834147]
212. Daggett V. α -sheet: The toxic conformer in amyloid diseases? *Accounts of Chemical Research.* 2006; 39:594–602. [PubMed: 16981675]
213. Beck DAC, Alonso DOV, Inoyama D, Daggett V. The intrinsic conformational propensities of the twenty naturally occurring amino acids and reflection of these propensities in proteins. *Proc. Natl. Acad. Sci. USA.* 2008; 105:12259–12264. [PubMed: 18713857]
214. Towse C-L, Vymetal J, Vondrasek J, Daggett V. Insights into unfolded proteins from the intrinsic ϕ/ψ propensities of the AAXAA host-guest series. *Biophysical Journal.* 2016; 110:348–361. [PubMed: 26789758]
215. Towse C-L, Hopping G, Vulovic I, & Daggett V. Nature versus design: The conformational propensities of D-amino acids and the importance of side chain chirality. *Protein Engineering, Design, and Selection.* 2014; 27:447–455.
216. Childers MC, Towse C-L, Daggett V. The effect of chirality and steric hindrance on intrinsic backbone conformational propensities: Tools for protein design. *Protein Engineering Design and Selection.* 2016; 29:271–280.
217. Towse C-L, Rysavy SJ, Vulovic IM, Daggett V. New Dynamic Rotamer Libraries: Data-Driven Analysis of Side Chain Conformational Propensities. *Structure.* 2016; 24:187–199. [PubMed: 26745530]
218. Childers MC, Towse CL, Daggett V. Molecular dynamics-derived rotamer libraries for D-amino acids, submitted for publication. 2016
219. Beck DAC, Jonsson AL, Schaeffer D, Scott KA, Day R, Toofanny RD, Alonso DOV, Daggett V. Dynameomics: Mass annotation of protein dynamics and unfolding in water by high-throughput atomistic molecular dynamics simulations. *Protein Engineering Design and Selection.* 2008; 21:353–368.
220. Van der Kamp MW, Anderson PC, Beck DAC, Benson NC, Jonsson AL, Merkle ED, Schaeffer RD, Scouras AD, Simms A, Toofanny RD, Daggett V. Dynameomics: A comprehensive database of protein dynamics. *Structure.* 2010; 18:423–435. [PubMed: 20399180]
221. Camilloni C, et al. Rational design of mutations that change the aggregation rate of a protein while maintaining its native structure and stability. *Sci Rep.* 2016; 6:25559. [PubMed: 27150430]
222. Fogolari F, et al. Molecular dynamics simulation suggests possible interaction patterns at 222 steps of beta2-microglobulin aggregation. *Biophys J.* 2007; 92:1673–1681. [PubMed: 17158575]
223. Esposito G, et al. The Controlling Roles of Trp60 and Trp95 in β 2-Microglobulin Function, Folding and Amyloid Aggregation Properties. *J. Mol. Biol.* 2008; 378:885–895.

Design, System, Application

Knowledge of the relationship between protein sequence, structure, dynamics, and function has resulted in the design of novel proteins and the optimization of existing ones. Dynamics often underlie the molecular mechanisms of protein stability and function. To this end, methods for accurately simulating the dynamics of proteins represent opportunities to improve protein designs. On such method, molecular dynamics (MD), uses physics-based energy functions and explicit representations of atomic systems to model protein dynamics. Such simulations can guide protein design efforts in several ways. First, by providing atomistic details of the molecular interactions that contribute to protein stability or protein function, simulations can directly guide the rational design of proteins. Second, by monitoring specific behaviors over the course of many simulations, MD can evaluate designed proteins to identify promising candidates for further study. In addition MD can provide information about target structures or properties unobtainable from static native structures. Finally, MD can be used to assess and screen computational designs. The explicit inclusion of protein dynamics in design strategies has the capacity to improve protein design while simultaneously contributing to our general understanding of the relationship between sequence, structure, dynamics, and function.

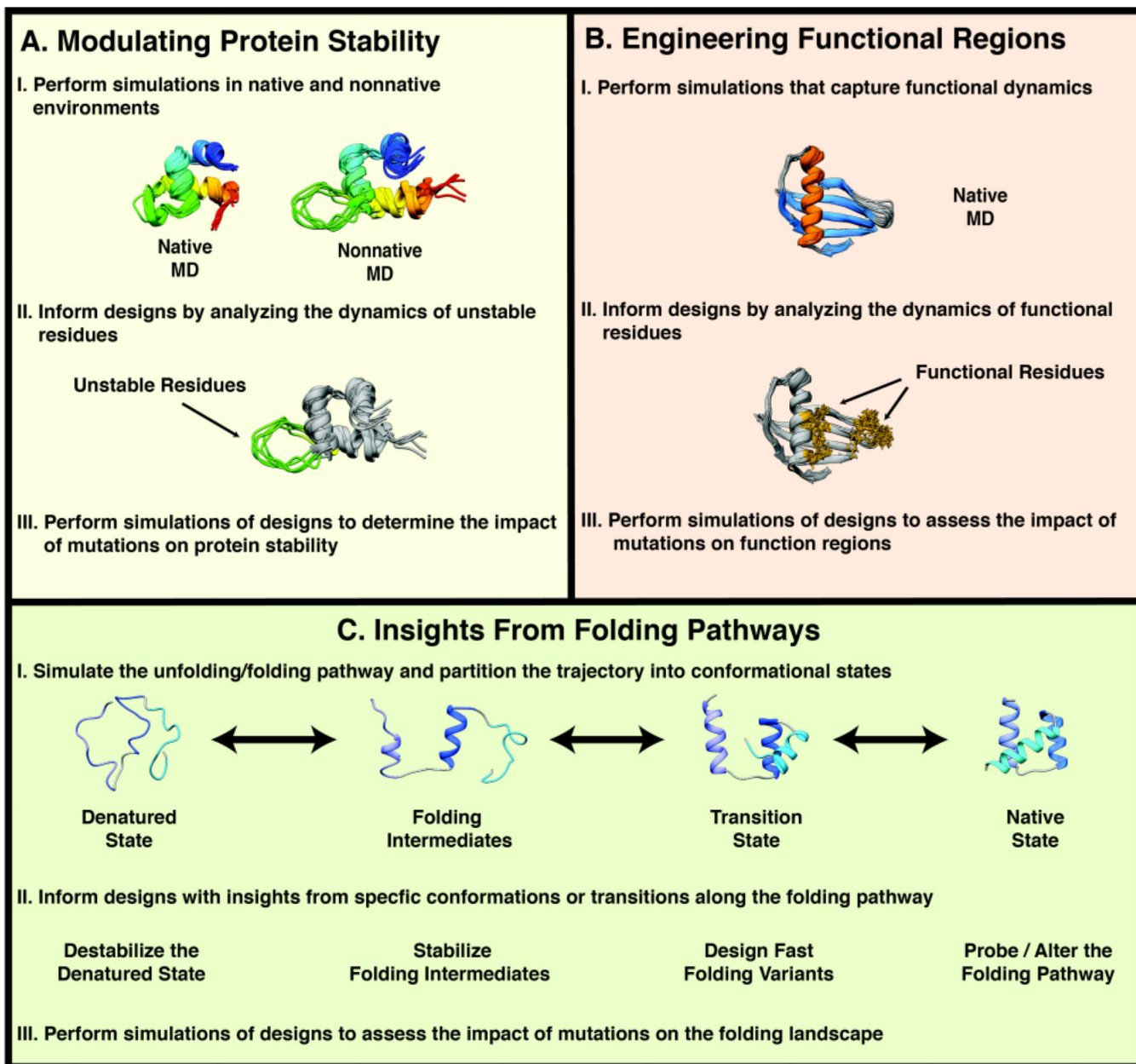


Figure 1. Applications of molecular dynamics for protein design
 Molecular dynamics simulations can be used to (A) design stable protein variants, (B) engineer functional regions, or (C) provide insights from protein unfolding / folding pathways.

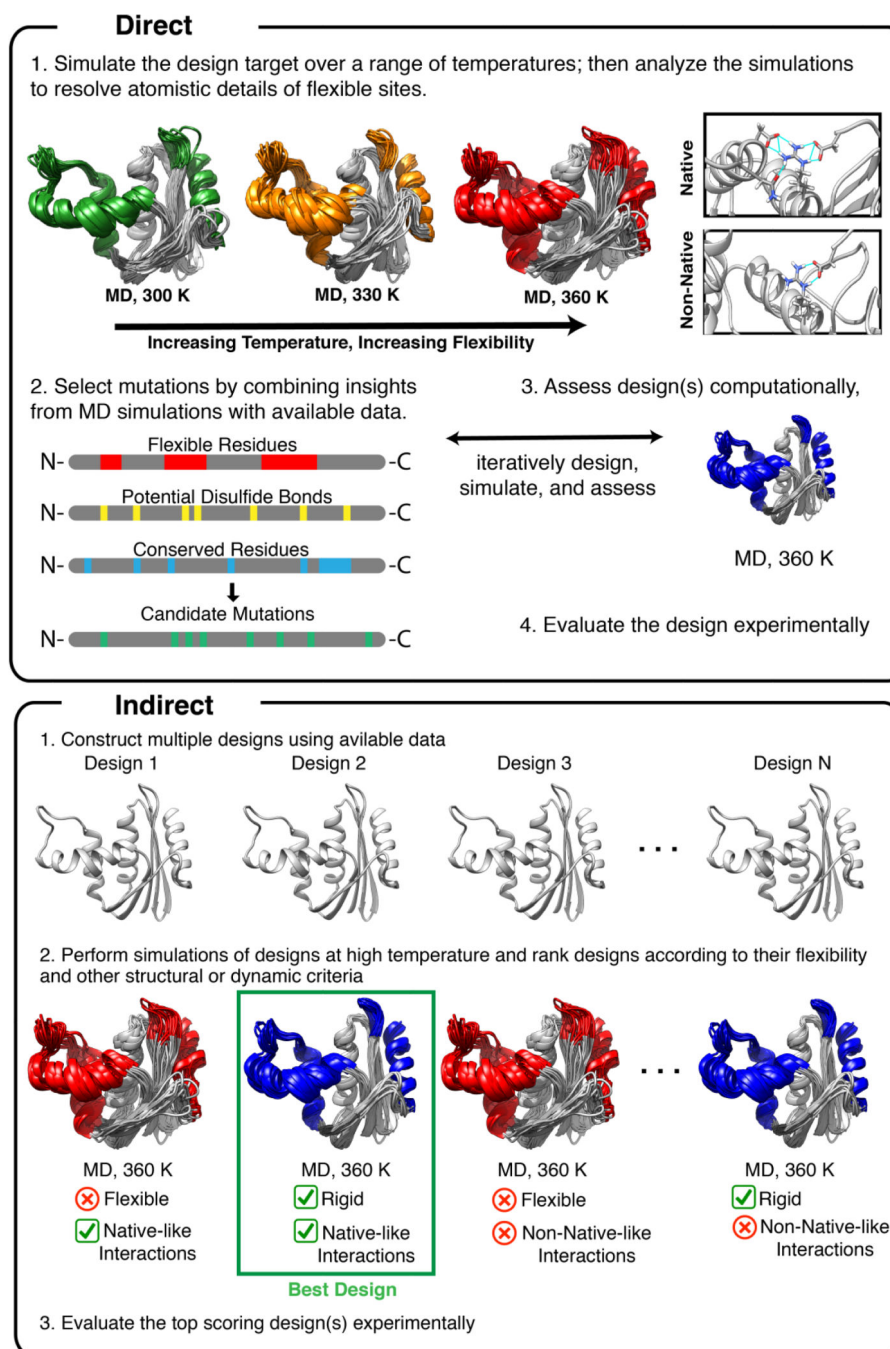


Figure 2. Overview of approaches to rigidify flexible regions of proteins

The rigidification of flexible sites is a common strategy for designing thermostable variants with MD simulations. In the direct application of the method, simulations are performed at various temperatures to identify regions of the protein that become flexible at high temperature. Interactions that underlie the increased flexibility at high temperature are identified by scrutinizing the trajectories. Then, proteins are designed (rationally or using other techniques) and simulated at high temperature to confirm that the designed variants are less flexible. In the indirect application of the method, high temperature simulations of

multiple designs are performed and the top performing designs are selected according to their satisfaction of pre-determined criteria such as the retention of native-like contacts or their flexibility at high temperature.

Author Manuscript

Author Manuscript

Author Manuscript

Author Manuscript

A. Structure of Wild Type Xylanase from *Bacillus circulans*

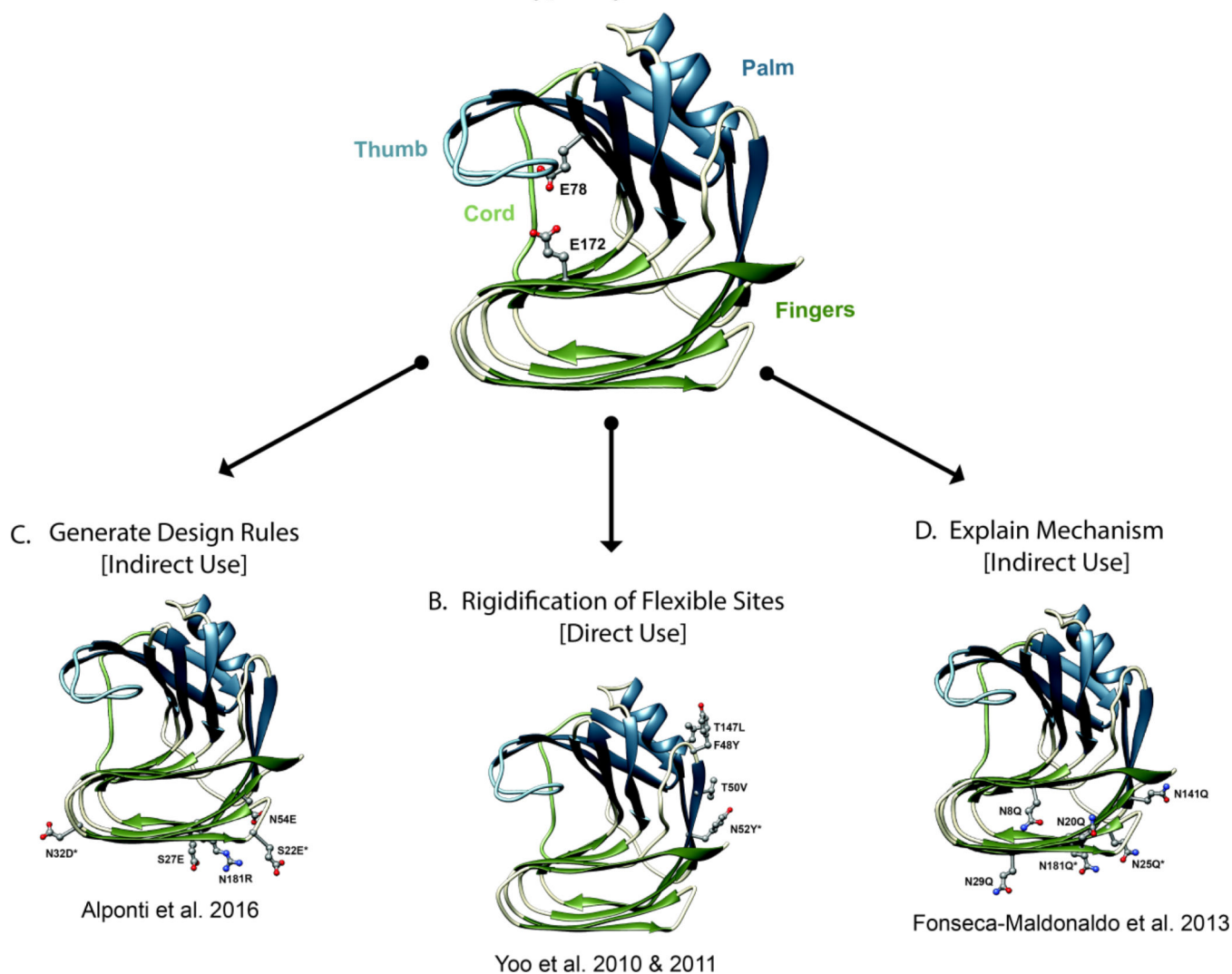


Figure 3. Molecular dynamics derived insights for designing stable xylanase variants

(A) The structure of wild type xylanase from *Bacillus circulans* is shown, colored according to the four structural regions that resemble a hand. The catalytic residues are shown as balls and sticks. Xylanase has been the subject of numerous protein design studies. (B) [Direct Use] Molecular dynamics simulations may be used to directly inform rational design efforts by predicting regions of the protein that become unstructured under destabilizing conditions, such as high temperature or low pH. The final design of Yoo and coworkers is shown in which MD simulations were used to inform the redesign of a flexible loop^{54,55}. (C) [Indirect Use] MD simulations may be used to generate rules for protein design. For example, the designed structure of Alponti et al. is shown, in which MD simulations of a thermophilic and mesophilic xylanase were compared to understand structural determinants of xylanase thermostabilization⁶⁵. (D) [Indirect Use] MD simulations may also be used to rationalize the mechanism of protein stabilization and in so doing, provide insights for optimizing designs. For example, shown is the final design of Fonseca-Maldonado et al. in which MD

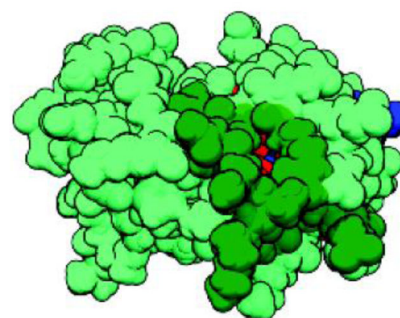
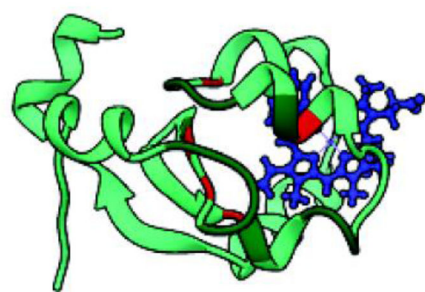
simulations of various glycosylation states of xylanase were used to rationalize the relationship between glycosylation and xylanase stability.

Author Manuscript

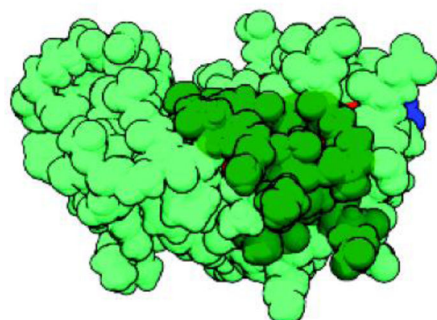
Author Manuscript

Author Manuscript

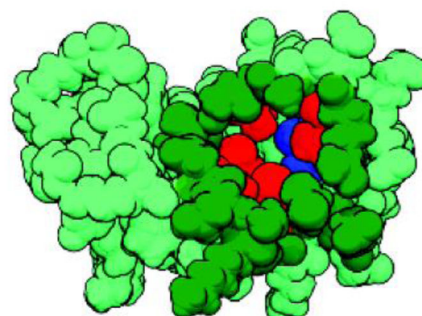
Author Manuscript



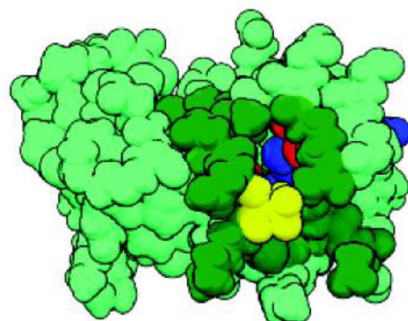
**WT, Crystal Structure
Closed**



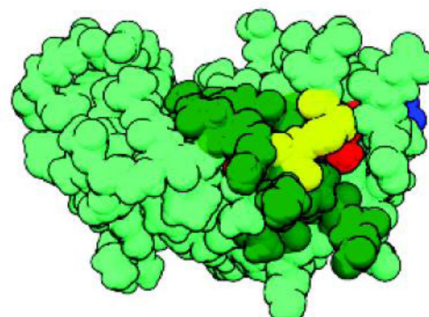
**WT, MD
Closed**



**WT, MD
Open**



**S18D, MD
Closed**



**S18C/R47C, MD
Closed**

Figure 4. Discovery of functional region in cytochrome b_5 by MD and subsequent computational design to regulate function

Cyclic opening and closing of a dynamic cleft providing access to the heme for electron transfer identified through MD simulations. Space-filling representations of cytochrome b_5 showing designed salt bridge to close the cleft (S18D) and introduction of disulfide bond (S18C/R47C). The buried hydrophobic residues that intermittently became exposed upon cleft formation are colored red. The heme group is colored blue.

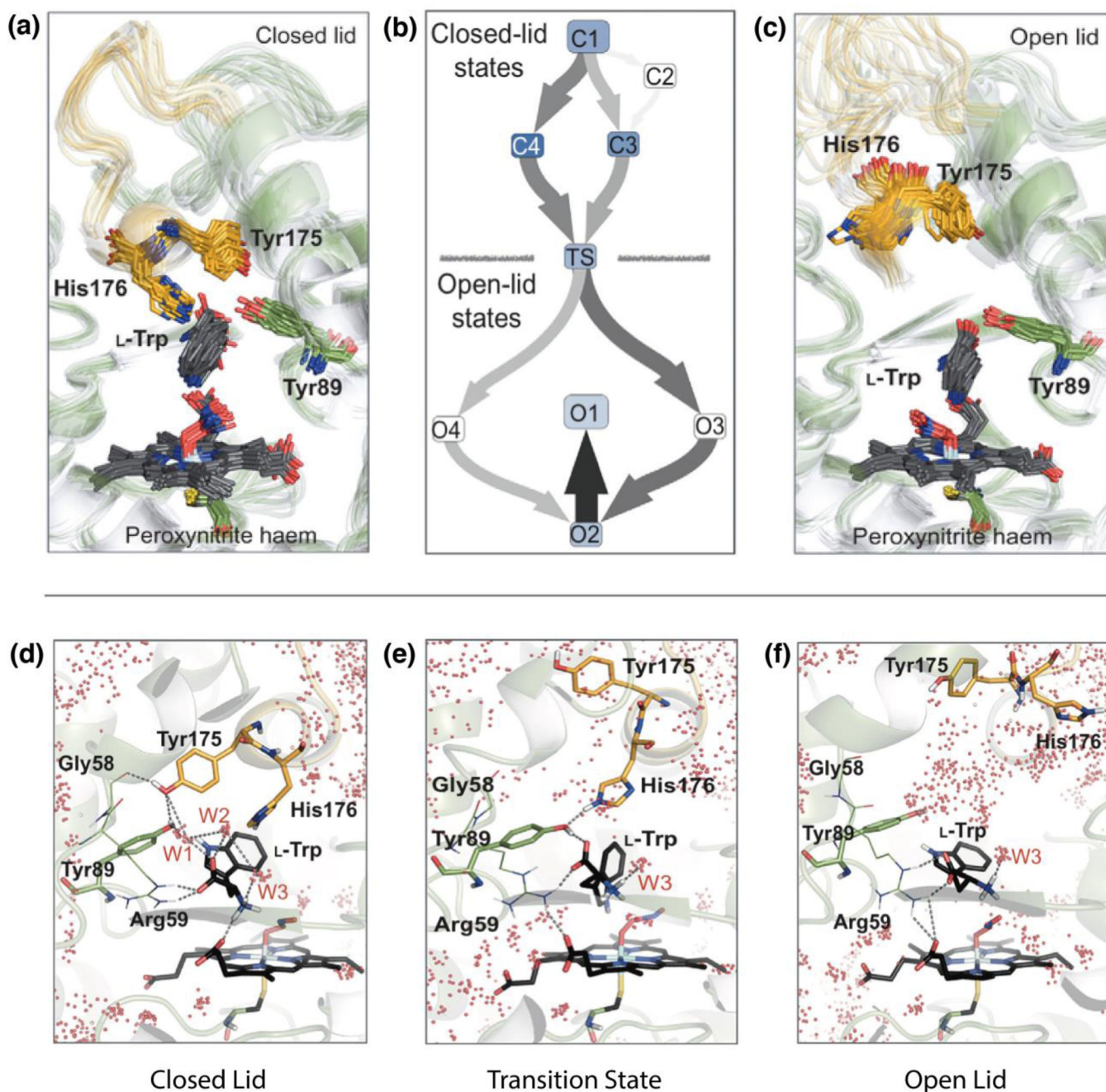


Figure 5. Identification of the opening/closing transition of the P450 TxtE F/G loop and engineering of regioselective Variants

P450 TxtE from *Streptomyces scabies* adopts both closed (a) and open (c) conformations of the F/G loop. Molecular dynamics simulations revealed the mechanism of conformational exchange between these two states, schematically illustrated in (b). In the open conformation, the binding pocket is exposed to solvent, which enables substrate (L-Trp) binding and product (4NT) release (f). In the closed conformation, water molecules (W1-3) and residues G58, Y175, and Y89 form a network of interactions that stabilize and orient substrate in the binding pocket (d). In the transition state, identified by MD, H176 and Y89

form transient interactions with substrate, which suggested that mutation of H176 would shift the conformational equilibrium between open and closed states when substrate is bound (e). *Figures reproduced from Dodani et al. 2016^{1,53}. Our panels a and c correspond to Figure 1b, panel b is Figure 2c, and panels 5d,e,f correspond to Figures 2a,b,d.*

Author Manuscript

Author Manuscript

Author Manuscript

Author Manuscript

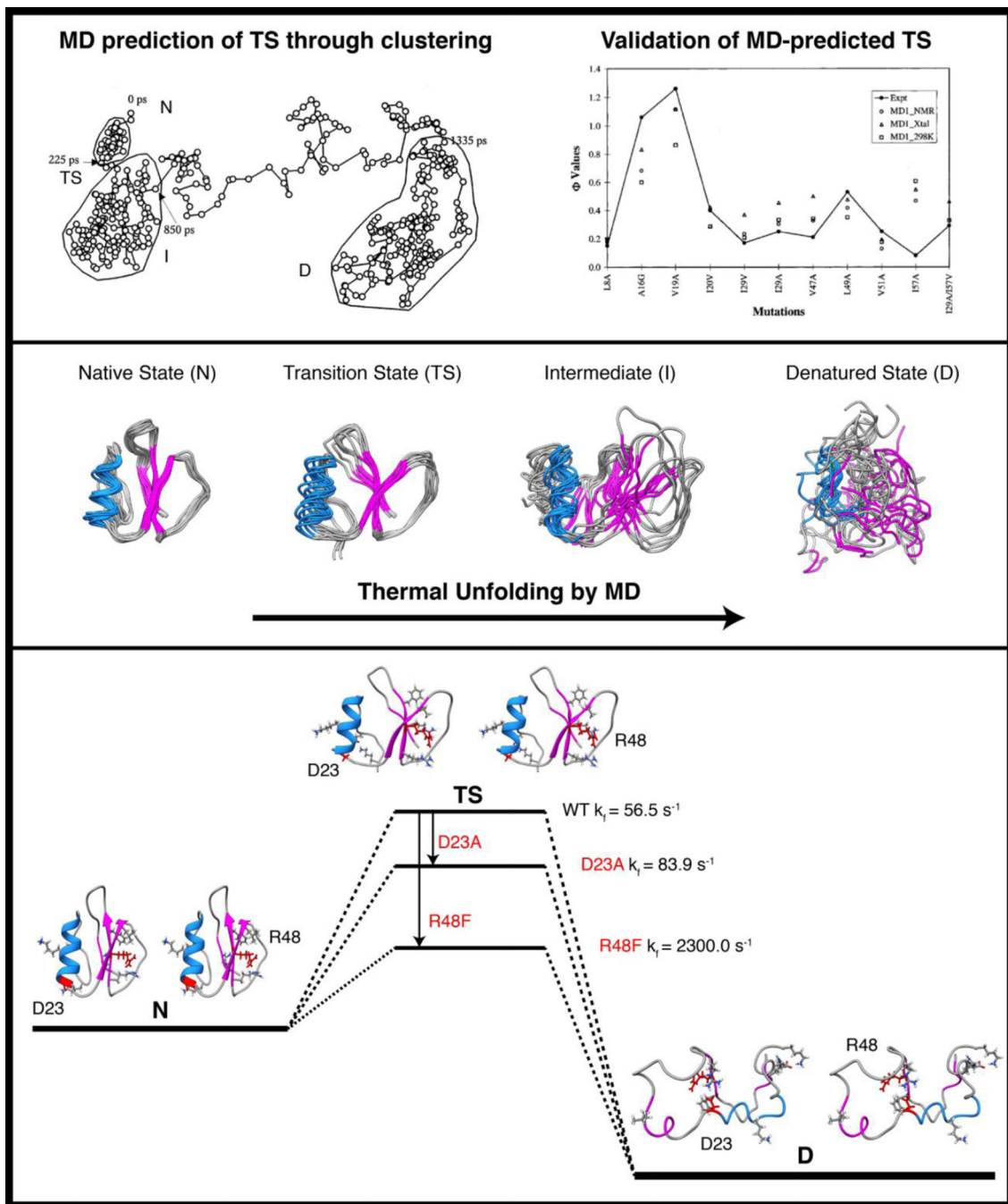


Figure 6. Thermal denaturation simulations to map unfolding pathways and characterize transition state structures for the rate-determining step of chymotrypsin inhibitor 2 (CI2)
 Top: Conformational clustering to identify putative TS regions and comparison of the identified structural ensembles with experiment (right). Center: Snapshots from different MD conformational ensembles are displayed highlighting the loss of structure and increased conformational sampling upon unfolding. Bottom: Interactions were identified in the MD-derived TS structures that could be improved upon with mutation while now affecting those same interactions in the native and denatured states. Designs were made and tested in silico and the predictions were validated by experiment. The goal of creating a faster folding

version of CI2 was realized through the designed mutations and the targeted interactions would not have been evident from static experimental structures or native state MD simulations.

Author Manuscript

Author Manuscript

Author Manuscript

Author Manuscript

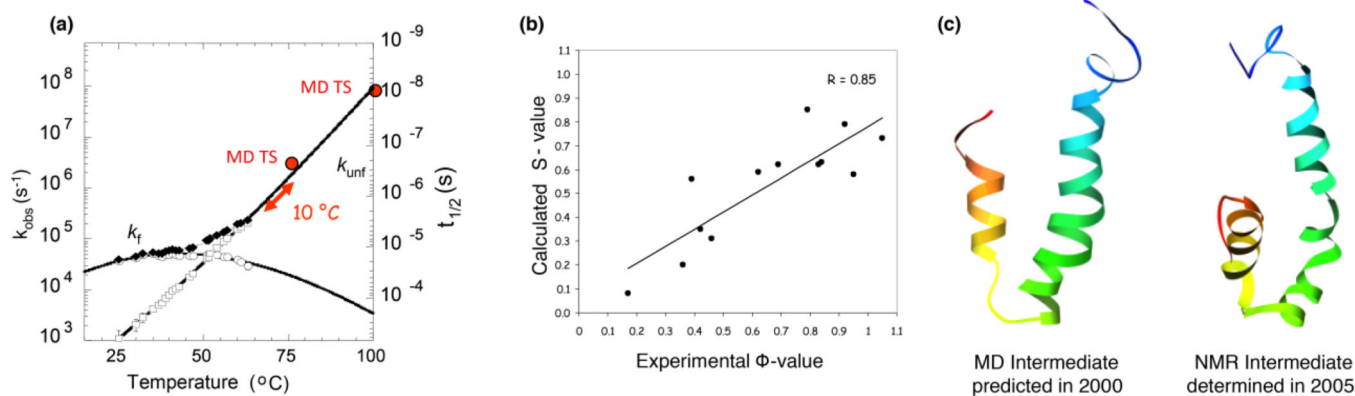


Figure 7. Experimental rates for unfolding and folding of the engrailed homeodomain (EnHD), along with MD-predicted TS times. Comparison of calculated S-values and experimental Φ -values, which both reflect the extent of structure for each residue probed, S-values through direct structure in the MD ensemble and Φ -values through inferred structure from ratios of free energies upon mutation. MD-predicted intermediate structure and NMR-derived intermediate structure determined several years later.

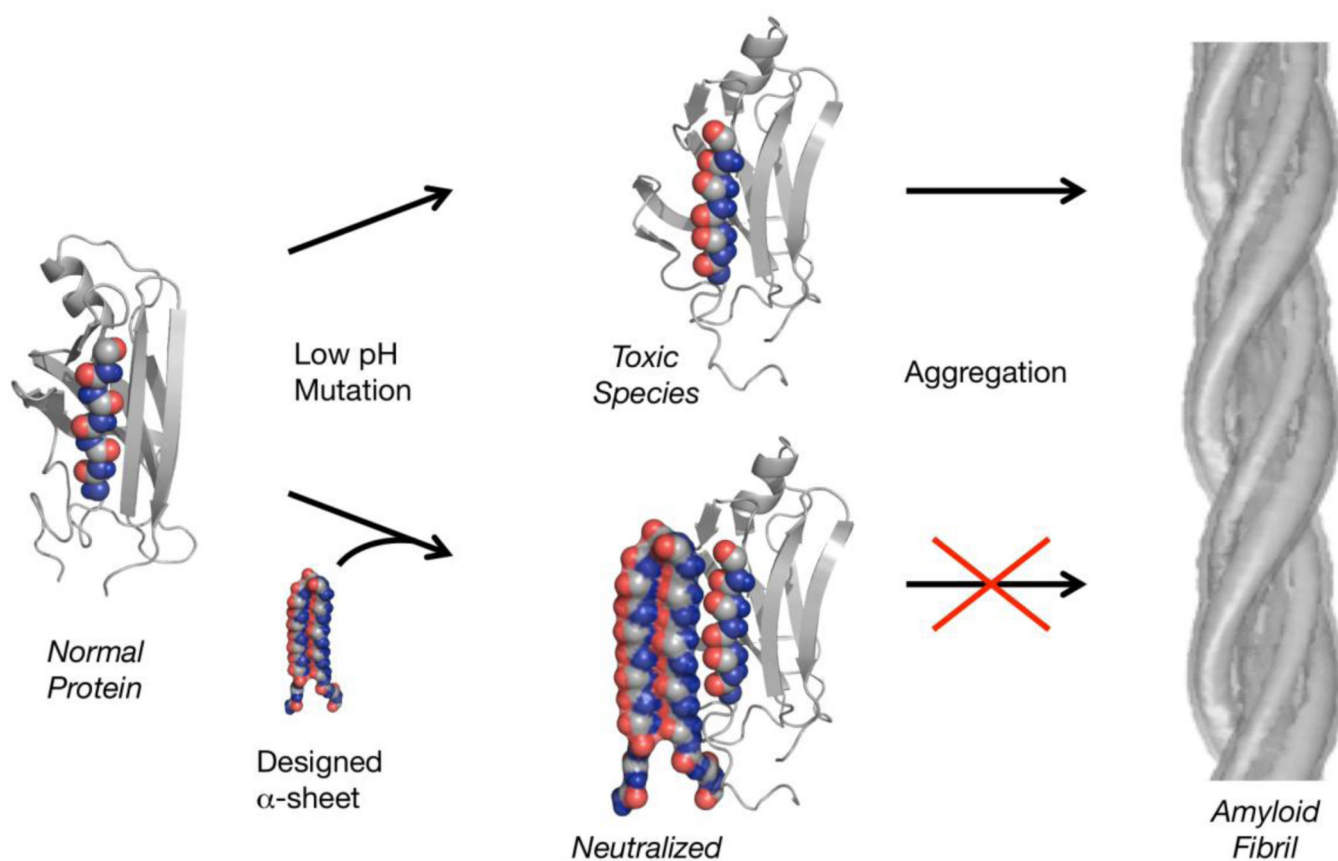


Figure 8. Schematic highlighting conversion of a β -strand in the amyloidogenic protein transthyretin at low pH to an α -strand with alignment of the carbonyl oxygens in red. Small α -sheet hairpins were designed to be complementary to the structure discovered through MD. Binding of the de novo designed α -sheet hairpin peptides inhibits aggregation and neutralizes toxicity associated with the soluble oligomers. Furthermore many amyloidogenic proteins and peptides adopt the α -sheet structure in MD and the same peptide designs cross react and inhibit aggregation in many amyloid disease systems.